WALKING ON THE UREIDE PATHWAY

PhD Course in Biochemistry and Molecular Biology

XXII cycle

2007-2009

Ilaria Lamberto

Department of Biochemistry and Molecular Biology
University of Parma, Italy

PhD Program Coordinator
Prof. Gian Luigi Rossi, Department of Biochemistry and Molecular Biology
University of Parma, Italy

Tutor
Prof. Riccardo Percudani, Department of Biochemistry and Molecular Biology
University of Parma, Italy

a G,

che nelle giornate di sole,
ma soprattutto nella tempesta
non ha mai lasciato la mia mano.

CONTENTS

Chapter 1

THE UREIDE PATHWAY

Physiological meaning of ureide accumulation

Ureide, allantoin and allantoate, are nitrogen-rich compounds derived from purine catabolism. The initial steps of purine degradation pathways converge on the production of xanthine, which is subsequently converted into uric acid (figure 1.1).
While birds, insects and most primates including humans, eliminate uric acid to get rid of excess nitrogen, for many others organisms the recovery of the purine ring nitrogen is vital. In microorganisms, amphibians and fish, uric acid is converted into urea and glyoxylate via allantoin and allantoate allowing the rescue of nitrogen atoms in environments where the availability of this element limits growth and life depends on efficient re-use of nitrogen atoms.

Product excreted or stored	Organisms
Guanine and /or xantine	molluscs
Uric acid	primates, reptiles, birds, molluscs, various insects, some terrestrial crustaceans
Allantoin	other mammals, various insects
Allantoic acid	various insects
Urea	microorganisms, some aquatic reptiles, terrestrial amphibians, teleost fishes
Ammonia	plants, aquatic amphibians, some insects, crustaceans

Table 1.1 Final product of ureide degradation in different organisms

Plant growth is often limited by nitrogen availability in the soil. While plants depend on efficient nitrogen uptake, they also require effective means to internally redistribute nitrogen during every stage of development [1]. Under agricultural conditions, nitrate and ammonia represent the predominant source of available nitrogen. In legumes, instead, nitrogen supply relies on N_2-fixation by symbiontic bacteria. For long distance translocation, ammonia which is the direct product of nitrogenase, is toxic and it must be converted in others nitrogenous compounds to be transported to the areal parts of the plant. To this end plants use either amides (asparagine and glutamine) or ureides (allantoin and allantoate), so legumes are classified as amide or ureide exporters according to the compounds used for the mobilization of fixed N [2]. Fixed nitrogen requires carbon skeletons for assimilation; one benefit to employ ureide is that one of this molecule contains four nitrogen atoms with a N:C ratio 1:1, higher than amide, although ureides are less soluble than amide [3]. In addition to the hypothesized advantage of ureides in terms of carbon use efficiency (N:C ratio), these molecules may provide the plant with greater control over nitrogen transport and metabolism. In lupine (an amide transporter) certain amino acids can be selectively removed from the xylem stream,

while others are selectively transferred to the phloem [4]. Thus the plant may control nitrogen metabolism by controlling the form of N metabolites. While asparagine is involved in many aspects of metabolism, ureides appear to serve only in nitrogen transport and storage. This 'specialization' may give the plant greater control of its nitrogen metabolism.

Ureides are the oxidation products of purines synthesized de *novo* in the root nodule [2]. The estimated ”metabolic cost" of ureide biosynthesis in ATP equivalents is less than 50% that of asparagine synthesis per N atom [2]; in theory, this allows the plant to invest relatively less energy in the production of nitrogen-transport compounds in the nodule and may provide a selective advantage to ureide-transporting plants.

Depending on growth requirements, ureides can accumulate or further metabolized in the endoplasmic reticulum [5]**,** making the nitrogen stored in the purine bases accessible for subsequent anabolic reactions.

The main tissue of ureides biosynthesis is the root nodule even if ureides are produced in seedling and leaves too. In higher plants ureide are detected in low concentrations in various tissues with the exception of senesced leaves a senescing cotyledons of both legumes and non-legume seedlings. In Arabidopsis seedlings, the accumulation of urea was partially inhibited by allopurinol [6], an inhibitor of xanthine dehydrogenase [7] [8], the enzyme that catalyses the oxidation of xanthine to uric acid.

Although much of the nitrogen released from ureides is ultimately stored in seed storage proteins, the primary site of ureide catabolism is the leaf [9]. There is little apparent storage of ureides in the leaf: the nitrogen released is allocated to leaf growth and maintenance, and to the synthesis of amino acids which are transported to the developing fruit or pods [10].

Purine catabolism and biosynthesis of ureides

In plant, a first step of purine catabolism occurs in the cytoplasm of infected nodule cells and leads to the production of oxopurines, such as hypoxanthine, xanthine and uric acid (figure 1.1). Uric acid is then transferred to uninfected cells into the peroxisome and further metabolized to allantoin.

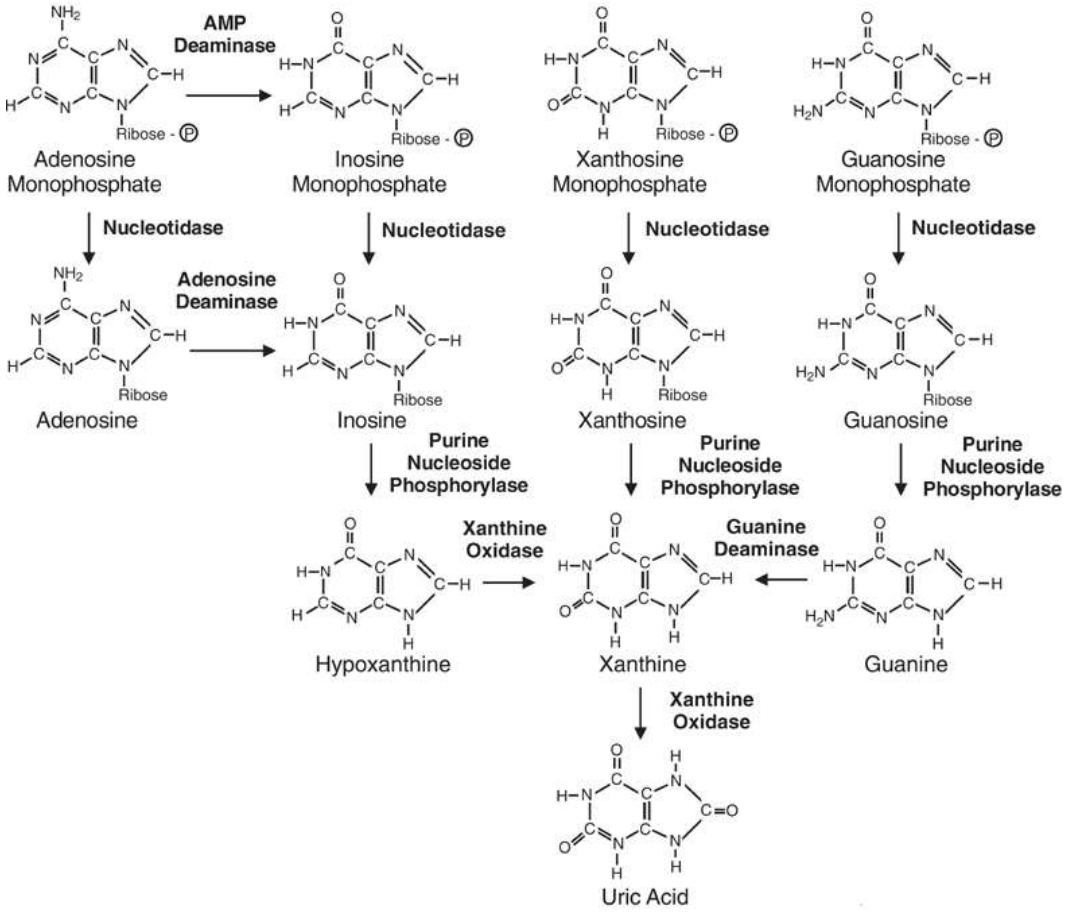

Figure 1.1 Biosynthesis of uric acid from purine bases (adapted from Navolanic et al. 2002) [11]

The conversion of uric acid into allantoin had long been thought to involve a single step catalyzed by urate oxidase (E.C. 1.7.3.3; uricase), but when the reaction was monitored directly by ^{13}C-NMR, the true product of the urate oxidase reaction was determined to be 5-hydroxyisourate (HIU) [12, 13]: urate oxidase catalyzes the conversion of urate to 5-hydroxyisourate (HIU), an unstable compound that, *in vitro*, decomposes spontaneously to 2-oxo-4-hydroxy-4-carboxy-5-ureidoimidazoline (OHCU); non-enzymatically decay of OHCU yield allantoin. The non-enzymatic decomposition of HIU generates a racemic mixture of allantoin with a half-time of hours. Soybean allantoinase is specific

for S-allantoin in vitro [14], and studies tracing the fate of ^{14}C-urate in soybean root nodules demonstrated that allantoin is produced stereospecifically [15] and that no allantoin racemase activity is present in the root nodule (Xu and Tipton, unpublished results).

In 2006 Ramazzina and co-workers completed the uric acid degradation pathway identifying the mouse genes coding for HIU hydrolase and OHCU decarboxylase. [16] (figure 2.1).

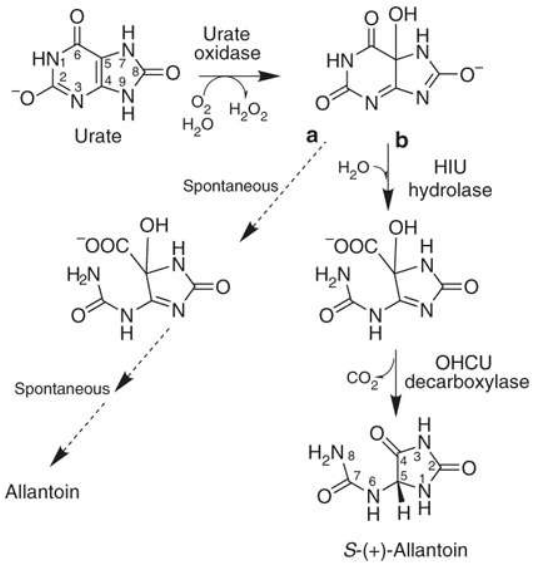

Figure 1.2 Synthesis of allantoin from uric acid.

A) Spontaneous degradation of HIU produces racemic allantoin. B) Enzymatic degradation of HIU by HIU hydrolase produces OHCU. OHCU can be decarboxylate to yield S-allantoin by OHCU decarboxylase. (Adapted from Ramazzina et al,2006) [16]

A gene encoding a protein with HIU hydrolase (HIUase) activity, related by homology to glucosidases has been described in soybean root nodules [17, 18], whereas a different HIUase, related to transthyretin, is encoded by bacterial (*pucM*) [19] and mammalian (*urah*) genes [16].

Genes encoding for OHCU decarboxylase are present in a variety of organisms, including bacteria, fungi, plants, and metazoa and are tightly associated with urate oxidase and HIU hydrolase and the product of these genes has been found to be required for the stereo-selective formation of S-allantoin that can be further hydrolized in the endoplasmic reticulum by allantoinase (E.C. 3.5.2.5) yield allantoate [20].

Allantoinase, which hydrolyze allantoin to allantoate, has been characterized from yeast (*Saccharomyces cerevisiae*) [21], *Arabidopsis*, [22] *Soybean* [14, 23, 24], *French bean* [25] and *Vigna* [26].

Desimone and co-workers [27] demonstrated that *Arabidopsis* could uptake and use allantoin as a sole nitrogen source. The absence of nitrogen in the medium increased the expression of the gene and the addition of allantoin to the medium as a sole source of nitrogen resulted in the up-regulation of the allantoinase gene [22].

Ureide catabolism and nitrogen rescue

In the upper parts of the plants (leaves, developing fruits and developing seeds) ureides must be converted into useful metabolic intermediates and the nitrogen-released assimilated into other nitrogen-containing molecules like aminoacids. Complete nitrogen utilization of allantoate requires that its two ureido groups be converted to ammonia.

The breakdown of allantoate can occur through two enzymes: allantoate amidinohydrolase (allantoicase) and allantoate amidohydrolase; allantoicase (EC 3.5.3.4) was identified first as the enzyme for the catabolism of allantoic acid leading to the production of urea and CO_2 [28] and does not require metal ions to work [29]. Allantoate amidohydrolase (EC 3.5.3.9), instead, did not produce urea but NH_4^+ and CO_2. [30] (figure 1.3). It was shown that allantoate amidohydrolase require manganese as a cofactor for active allantoic acid degradation [31].

Both allantoicase and allantoate amidohydrolase are present in the soybean germplasm and different cultivars may contain one pathway exclusively or both [32]. This difference is thought to have agronomic importance, as the allantoicase is believed continue to degrade allantoate under water-limiting conditions, preventing the build-up of ureides and subsequent inhibition of nitrogen fixation. Conversely, the amidohydrolase is believed to become inactive under water-defcit, ultimately contributing to the inhibition of nitrogen fixation [32, 33] . Allantoate amidohydrolase has been shown to require manganese for activity in vitro [30] and in planta [31] and manganese has been implicated in the tolerance of nitrogen fixation to drought [34]. The presence of magnesium, calcium, iron, cobalt, and nickel, instead, does not activate the enzyme.

The addition of metal chelators like EDTA and acetohydroxamate abolished the hydrolase activity; [35, 36] borate [35] and L-Asn [31] were shown to inhibit allantoate-degrading activity in soybean extracts, and both inhibitors were postulated to function by chelating manganese [31]. The inhibition of allantoate-degrading activity by L-Asn may be of physiological relevance: upon application of mineral nitrogen [37] or during drought stress [38] ureide accumulation in leaves is observed and coincides with the shutdown of nitrogen fixation in the nodules; also, under these conditions, the L-Asn concentration in the shoot rises drastically, and it was postulated that either L-Asn or the accumulating ureides serve as feedback signal for the reduction of nitrogen fixation [39].

Allantoate degradation produces ureidoglycolate, which is metabolized to glyoxylate by the enzymes ureidoglycolate urea-lyase (EC 4.3.2.3) or ureidoglycolate amidohydrolase (EC 3.5.3.19). Both a

ureidoglycolate amidohydrolase (EC 3.5.3.19) [25] and a ureidoglycolate urea-lyase (EC 4.3.2.3) [40] have been purified from French bean and other leguminous species. Ureidoglycolate urea-lyase, produces urea, whereas ureidoglycolate amidohydrolase, produces and NH_4^+ and CO_2 (figure 1.3).

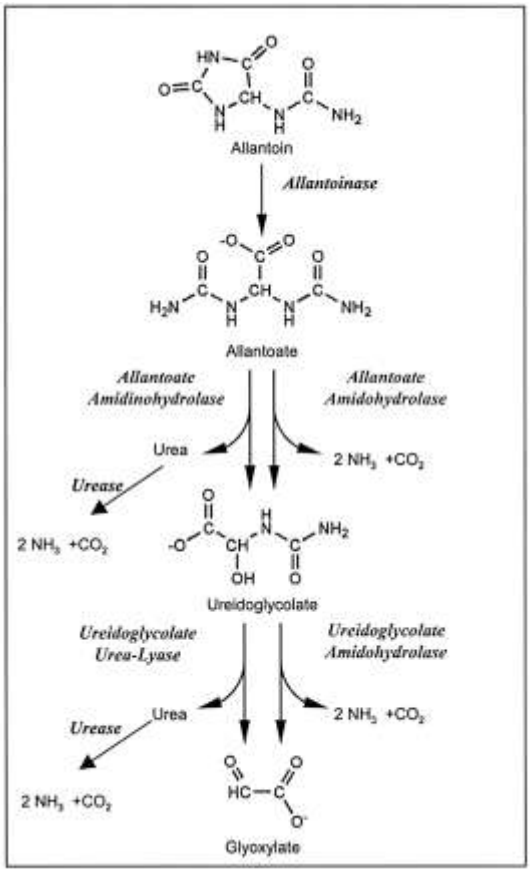

Figure1.3 Different way in nitrogen rescue on the ureide pathway

Subcellular localization of ureide metabolism enzymes

In previous studies to investigate the subcellular localization of the enzymes involved in the ureide pathway using sucrose gradient centrifugation on cellular extracts, xanthine dehydrogenase was found in the cytosol, uricase in the peroxisome, allantoinase was assigned to the microsomal endoplasmic reticulum (ER) fraction, although a peroxisomal origin of the microsomes could not be excluded [20] and an ureidoglycolate amidohydrolase activity from French bean was associated with the peroxisome [25]. Immunocytochemical methods localized uricase [41] as well as hydroxyisourate hydrolase [18] exclusively to the peroxisomes of uninfected nodule cells. In animals, uricase is also localized to the peroxisome, whereas allantoinase was found in the peroxisome or the cytosol in fish but in the mitochondria in amphibians [42]. The subcellular localization of recombinant allantoinase

and allantoate amidohydrolase (AAH) have been determined in *Arabidopsis* and soybean. Fluorescent fusion proteins of allantoinase and both allantoate amidohydrolases localize to the endoplasmic reticulum after transient expression and in transgenic plants [5].

Ureide, drought stress and N_2 fixation

Nitrogen fixation is sensitive to water-deficit stress [43]. Although N_2 fixation decreases during drought, the products of N_2 fixation, ureides, increase in leaves of drought-sensitive soybean genotypes [44].

Under well-watered conditions and high leaf water potentials, ureide concentration is very low in nodule, root, and leaf-blade tissues. During soil dehydration leaf water potential decreased substantially, indicating a fairly severe level of drought stress, and it is associated with an accumulation of ureides in the leaf blades and nodules. The shoot ureides increase [32, 45] is due to a decreased rate of ureide catabolism in leaves [29, 38].

Despite research effort in the area, the mechanisms influencing N_2 fixation in response to limited soil water are not well understood. Accumulating evidence indicates that the decline in N_2 fixation during water deficits may be associated with levels of nitrogenous compounds, such as amino acids or ureides, in leaves or nodules of N_2-fixing plants [32, 34, 38, 46]. How specific compounds regulate nodule activity is unclear, although several hypotheses have been proposed [43].

It has been speculated that ureides are closely involved in a feedback mechanism between decreased their catabolism in the shoot and inhibition of N_2 fixation in the nodules [38].

Leaf ureides and nodule asparagine do not feedback inhibit N_2 fixation. The potential candidates for feedback inhibition of N_2 fixation by reducing the nitrogenase activity include nodule ureides, nodule aspartate, and several amino acids in leaves.

Physiological studies have demonstrated that increases in Mn^{2+} availability to the plant during water-deficit stress increases ureide degradation in leaves and prolongs N_2 fixation [32, 34]. It was shown that lower ureide concentrations in leaves during water-deficit stress appears to prolong N_2 fixation and thereby to confer drought tolerance [34, 47].

This may be correlate to the allantoate amidohydrolase that requires Mn^{2+} as a co-factor for activity [5, 31]. This enzyme has greater activity in Jackson, a drought-tolerant N_2-fixation soybean genotype, than in the drought-sensitive genotype KS4895 [34].

The pathway of allantoic acid degradation in leaves may be important in determining the sensitivity of N_2 fixation to drying soil. The allantoate amidinohydrolase pathway appears to be generally advantageous in conferring drought tolerance, especially under soil conditions where the availability of Mn^{2+} was low. Plants with the allantoate amidohydrolase pathway when supplied Mn^{2+}, had high degradation rates and N_2 fixation with increased tolerance to water deficits. Consequently, both genetic selection of the ureide degradation pathway and improved management of soil Mn^{2+} availability appear to be viable approaches to minimize the deleterious consequences of inhibited N_2 fixation activity with drying soils. Exogenous ureides applied to the soil and water-deficit treatments

inhibited N_2 fixation by 85% to 90%. Mn^{2+} fertilization increased the apparent catabolism of ureides in leaves and hastened the recovery of N_2 fixation following exogenous ureide application for both cultivars.

Ureides and total free amino acids in leaves and nodules increase during water deficits and coincide with a decline in N_2 fixation. It was hypothesized that Asn chelates Mn, thereby inhibiting allantoate amidohydrolase and allantoate catabolism [31].

REFERENCES

1. Rentsch, D., S. Schmidt, and M. Tegeder, *Transporters for uptake and allocation of organic nitrogen compounds in plants.* FEBS Lett, 2007. **581**(12): p. 2281-9.
2. Schubert, K.R., *Products of Biological Nitrogen Fixation in Higher Plants: Synthesis, Transport, and Metabolism*. 1986. p. 539-574.
3. Layzell, D.B., et al., *Economy of Photosynthate Use in Nitrogen-fixing Legume Nodules: Observations on Two Contrasting Symbioses.* Plant Physiol, 1979. **64**(5): p. 888-891.
4. McNeil, D.L., C.A. Atkins, and J.S. Pate, *Uptake and Utilization of Xylem-borne Amino Compounds by Shoot Organs of a Legume.* Plant Physiol, 1979. **63**(6): p. 1076-1081.
5. Werner, A.K., et al., *Identification, biochemical characterization, and subcellular localization of allantoate amidohydrolases from Arabidopsis and soybean.* Plant Physiol, 2008. **146**(2): p. 418-30.
6. Zonia, L.E., N.E. Stebbins, and J.C. Polacco, *Essential role of urease in germination of nitrogen-limited Arabidopsis thaliana seeds.* Plant Physiol, 1995. **107**(4): p. 1097-103.
7. Triplett, E.W., D.G. Blevins, and D.D. Randall, *Allantoic Acid Synthesis in Soybean Root Nodule Cytosol via Xanthine Dehydrogenase.* Plant Physiol, 1980. **65**(6): p. 1203-1206.
8. Leydecker, M.T., et al., *Molybdenum Cofactor Mutants, Specifically Impaired in Xanthine Dehydrogenase Activity and Abscisic Acid Biosynthesis, Simultaneously Overexpress Nitrate Reductase.* Plant Physiol, 1995. **107**(4): p. 1427-1431.
9. Pate, J.S. and C.A. Atkins, *Xylem and Phloem Transport and the Functional Economy of Carbon and Nitrogen of a Legume Leaf.* Plant Physiol, 1983. **71**(4): p. 835-840.
10. Peoples, M.B., et al., *Nitrogen Nutrition and Metabolic Interconversions of Nitrogenous Solutes in Developing Cowpea Fruits.* Plant Physiol, 1985. **77**(2): p. 382-388.
11. Navolanic, P.M., et al., *Elitek-rasburicase: an effective means to prevent and treat hyperuricemia associated with tumor lysis syndrome, a Meeting Report, Dallas, Texas, January 2002.* Leukemia, 2003. **17**(3): p. 499-514.
12. Kahn, K. and P.A. Tipton, *Kinetic mechanism and cofactor content of soybean root nodule urate oxidase.* Biochemistry, 1997. **36**(16): p. 4731-8.
13. Modric, N., et al., *Tracing and identification of uricase. Reaction intermediates.: A direct 13C-NMR/isotope-labelling evidence.* Tetrahedron Letters, 1992. **33**(44): p. 6691-6694.
14. Lee, K.W. and A.H. Roush, *Allantoinase Assays and Their Application to Yeast and Soybean Allantoinases.* Arch Biochem Biophys, 1964. **108**: p. 460-7.
15. Kahn, K. and P.A. Tipton, *Kinetics and Mechanism of Allantoin Racemization.* Bioorganic Chemistry, 2000. **28**(2): p. 62-72.
16. Ramazzina, I., et al., *Completing the uric acid degradation pathway through phylogenetic comparison of whole genomes.* Nat Chem Biol, 2006. **2**(3): p. 144-8.
17. Sarma, A.D., et al., *Identification and purification of hydroxyisourate hydrolase, a novel ureide-metabolizing enzyme.* J Biol Chem, 1999. **274**(48): p. 33863-5.
18. Raychaudhuri, A. and P.A. Tipton, *Cloning and expression of the gene for soybean hydroxyisourate hydrolase. Localization and implications for function and mechanism.* Plant Physiol, 2002. **130**(4): p. 2061-8.
19. Lee, Y., et al., *Transthyretin-related proteins function to facilitate the hydrolysis of 5-hydroxyisourate, the end product of the uricase reaction.* FEBS Lett, 2005. **579**(21): p. 4769-74.
20. Hanks, J.F., N.E. Tolbert, and K.R. Schubert, *Localization of Enzymes of Ureide Biosynthesis in Peroxisomes and Microsomes of Nodules.* Plant Physiol, 1981. **68**(1): p. 65-69.
21. Buckholz, R.G. and T.G. Cooper, *The allantoinase (DAL1) gene of Saccharomyces cerevisiae.* Yeast, 1991. **7**(9): p. 913-23.
22. Yang, J. and K.H. Han, *Functional characterization of allantoinase genes from Arabidopsis and a nonureide-type legume black locust.* Plant Physiol, 2004. **134**(3): p. 1039-49.

23. Webb, M.A. and J.S. Lindell, *Purification of allantoinase from soybean seeds and production and characterization of anti-allantoinase antibodies.* Plant Physiol, 1993. **103**(4): p. 1235-41.

24. Bell, J.A. and M.A. Webb, *Immunoaffinity purification and comparison of allantoinases from soybean root nodules and cotyledons.* Plant Physiol, 1995. **107**(2): p. 435-41.

25. Wells, X.E. and E.M. Lees, *Ureidoglycolate amidohydrolase from developing French bean fruits (Phaseolus vulgaris [L.].).* Arch Biochem Biophys, 1991. **287**(1): p. 151-9.

26. Subhash Reddy, R., N. Venkateswara Rao, and K. Sivarama Sastry, *Acetohydroxamate, a competitive inhibitor of allantoinases of Vigna radiata.* Phytochemistry, 1989. **28**(1): p. 47-49.

27. Desimone, M., et al., *A novel superfamily of transporters for allantoin and other oxo derivatives of nitrogen heterocyclic compounds in Arabidopsis.* Plant Cell, 2002. **14**(4): p. 847-56.

28. Shelp, B.J. and R.J. Ireland, *Ureide Metabolism in Leaves of Nitrogen-Fixing Soybean Plants.* Plant Physiol, 1985. **77**(3): p. 779-783.

29. Vadez, V. and T.R. Sinclair, *Leaf ureide degradation and N(2) fixation tolerance to water deficit in soybean.* J Exp Bot, 2001. **52**(354): p. 153-9.

30. Winkler, R.G., et al., *Ureide Catabolism of Soybeans : II. Pathway of Catabolism in Intact Leaf Tissue.* Plant Physiol, 1987. **83**(3): p. 585-591.

31. Lukaszewski, K.M., D.G. Blevins, and D.D. Randall, *Asparagine and Boric Acid Cause Allantoate Accumulation in Soybean Leaves by Inhibiting Manganese-Dependent Allantoate Amidohydrolase.* Plant Physiol, 1992. **99**(4): p. 1670-1676.

32. Vadez, V. and T.R. Sinclair, *Ureide degradation pathways in intact soybean leaves.* J Exp Bot, 2000. **51**(349): p. 1459-65.

33. Sinclair, T.R., V. Vadez, and K. Chenu, *Ureide accumulation in response to Mn nutrition by eight soybean genotypes with N-2 fixation tolerance to soil drying.* Crop Science, 2003. **43**(2): p. 592-597.

34. Purcell, L.C., C.A. King, and R.A. Ball, *Soybean Cultivar Differences in Ureides and the Relationship to Drought Tolerant Nitrogen Fixation and Manganese Nutrition*. 2000. p. 1062-1070.

35. Winkler, R.G., et al., *Enzymic Degradation of Allantoate in Developing Soybeans.* Plant Physiol, 1985. **79**(3): p. 787-793.

36. Raso, M.J., et al., *Biochemical characterisation of an allantoate-degrading enzyme from French bean (Phaseolus vulgaris): the requirement of phenylhydrazine.* Planta, 2007. **226**(5): p. 1333-42.

37. Methode, B. and E.H. James, *The feedback mechanism of nitrate inhibition of nitrogenase activity in soybean may involve asparagine and/or products of its metabolism*. 1997. p. 371-377.

38. Serraj, R., et al., *Involvement of ureides in nitrogen fixation inhibition in soybean.* Plant Physiol, 1999. **119**(1): p. 289-96.

39. Todd, C.D. and J.C. Polacco, *AtAAH encodes a protein with allantoate amidohydrolase activity from Arabidopsis thaliana.* Planta, 2006. **223**(5): p. 1108-13.

40. Munoz, A., et al., *Urea is a product of ureidoglycolate degradation in chickpea. Purification and characterization of the ureidoglycolate urea-lyase.* Plant Physiol, 2001. **125**(2): p. 828-34.

41. Webb MA, N.E., *Cellular compartmentation of ureide biogenesis in root nodules of cowpea (Vigna unguiculata (L.) Walp.). .* Planta 1987. **172 .** p. 162–175.

42. Hayashi, S., S. Fujiwara, and T. Noguchi, *Evolution of urate-degrading enzymes in animal peroxisomes.* Cell Biochem Biophys, 2000. **32 Spring**: p. 123-9.

43. Serraj, R., T. Sinclair, and L. Purcell, *Review article. Symbiotic N2 fixation response to drought*. 1999. p. 143-155.

44. King, C.A. and L.C. Purcell, *Soybean Nodule Size and Relationship to Nitrogen Fixation Response to Water Deficit*. 2001. p. 1099-1107.

45. de Silva, M., L.C. Purcell, and C.A. King, *Soybean Petiole Ureide Response to Water Deficits and Decreased Transpiration*. 1996. p. 611-616.

46. R, P., et al., *Nodule growth and activity may be regulated by a feedback mechanism involving phloem nitrogen*.* 1993. p. 125-136.

47. King, C.A. and L.C. Purcell, *Inhibition of N2 fixation in soybean is associated with elevated ureides and amino acids.* Plant Physiol, 2005. **137**(4): p. 1389-96.

Chapter 2

S-ALLANTOIN SYNTHASE

S-allantoin synthase

ABSTRACT

S-allantoin, a major ureide compound, is produced in plant peroxisomes through degradation of oxidised purines. Fundamental information is missing on the enzymes and regulation of the plant pathway. Sequence evidence had suggested that the *TTL* gene product, a protein known as an interactor of brassinosterod receptors, may function as a bi-functional enzyme in the synthesis of S-allantoin. Here it is demonstrate that the recombinant TTL protein from *A. thaliana* catalyzes two enzymatic reaction leading to the steroselective formation of S-allantoin: hydrolysis of hydroxyisourate through a C-terminal Urah domain and decarboxylation of OHCU through a N-terminal Urad domain. Two different mRNAs are produced from the *TTL* gene through alternative use of two splice acceptor sites. The corresponding proteins differ for the presence (TTL^{1-}) and the absence (TTL^{2-}) of a central region containing a rare internal peroxisomal targeting signal (PTS2). The two proteins have similar catalytic activity *in vitro* but different *in vivo* localisation: TTL^{1-} localizes in peroxisomes whereas TTL^{2-} localizes in the cytosol. Transcripts deriving from the two splice variants are present in a similar proportion in various *Arabidopsis* tissues but in floral buds, where TTL^{2-} is prevalent. Analyses of TTL transcripts in various plants indicate that similar splice variants are present in monocots and dicots. The presence of this gene in all viridiplantae indicates that S-allantoin biosynthesis has general significance in plant nitrogen metabolism, while conservation of alternative splicing suggests that this mechanism have general implications in the regulation of the ureide pathway in flowering plants.

INTRODUCTION

In the ureide pathway, the conversion of uric acid into allantoin had long been thought to involve a single step catalyzed by urate oxidase (E.C. 1.7.3.3; uricase), but other investigations have revealed that this pathway includes two additional, distinct, chemically labile intermediates: 5-hydroxyisourate (HIU) and 2-oxo-4-hydroxy-4-carboxy-5-ureidoimidazoline (OHCU) [1].
The true product of the urate oxidase (Uox) reaction is found to be HIU, and its hydrolysis product, OHCU, is un intermediate in the formation of allantoin [1].
In 2006 Percudani's group identified two proteins associate to the enzymatic activity involved in the passage that produce allantoin from uric acid: HIU hydrolase and OHCU decarboxylase [2].
A gene encoding a protein with HIU hydrolase (HIUase) activity, related by homology to glucosidases has been described in soybean root nodules [3, 4], whereas a different HIUase, related to transthyretin, is encoded by bacterial (*pucM*) [5] and mammalian (*urah*) genes [2].
Genes encoding for OHCU decarboxylase are present in a variety of organisms, including bacteria, fungi, plants, and metazoa and are tightly associated with urate oxidase and HIU hydrolase and the product of these genes has been found to be required for the stereo-selective formation of S-allantoin [2]. Remarkably, it has been shown that the thyroid hormone transporter transthyretin originated in vertebrate by duplication of the *urah* gene[6]. Such finding implies that very different roles, such as enzymatic activities and hormone transport can be accomplished by the HIUase fold.
In the *Arabidopsis* genome is present one transthyretin-like gene (*TTL*) which encodes a protein with homology to Urah and Urad domains [2].
Interestingly, biochemical and genetic studies provided evidence that this protein is a potential substrate of the brassinosteroid (BR) receptor kinase at the plasma membrane, and it has been hypothesized that in *Arabidopsis* TTL behaves as a negative regulator in BR-mediated plant growth [7].

RESULTS AND DISCUSSION

Structure of the *Arabidopsis* TTL gene and its identification as a putative bi-functional HIU hydrolase-OHCU decarboxylase.

Comparison of the amino acid sequence of *A. thaliana* TTL with Urad and Urah proteins from zebrafish shows that TTL is a bi-domain protein containing a Urad domain at the N terminus and a Urah domain at the C terminus (figure 2.1).

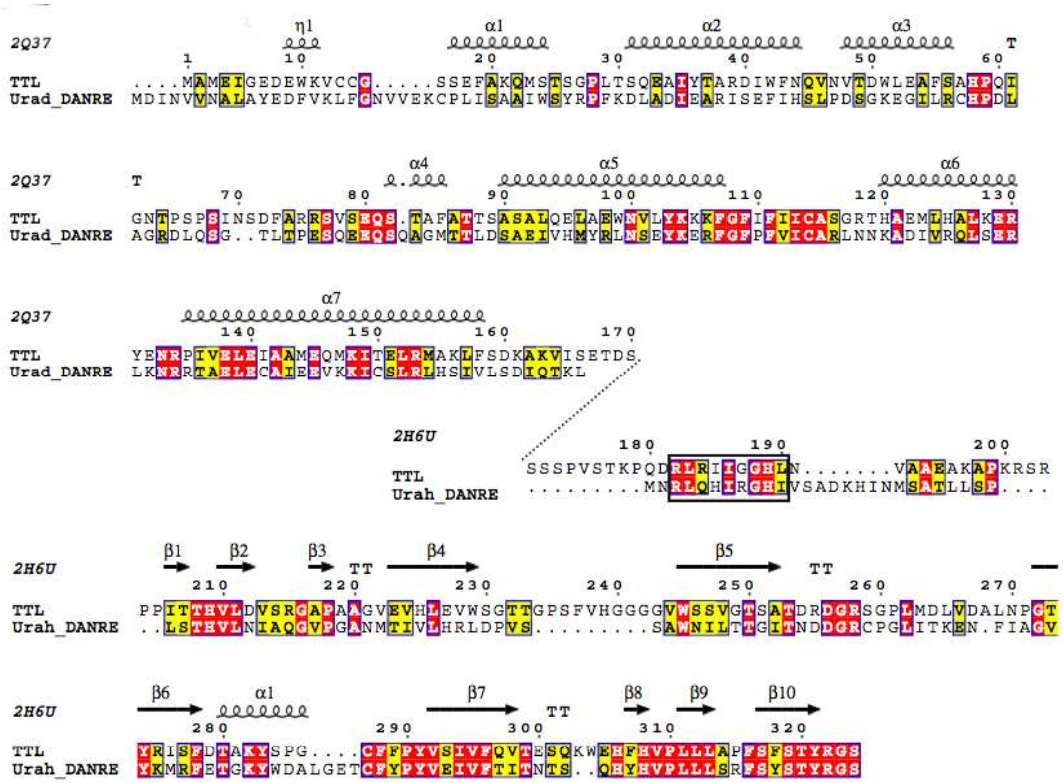

Figure 2.1 Sequence comparison suggest a role for TTL in allantoin biosynthesis. TTL is a bi-domain protein containing a Urad domain at the N terminus and a Urah domain at the C terminus The sequence motif corresponding to the PTS2 consensus is boxed. Secondary structure elements derived from the three dimensional coordinates of the Urad domain from *A. thaliana* [8] and the Urah domain from zebrafish [6] are drown above the alignment.

Two TTL variants differing by the presence of an internal peroxisomal targeting signal are produced by alternative splicing.

EST analysis of TTL transcripts suggest the presence of alternative splice forms of this gene [9].
A single strand cDNA was generated using RNA extracted from *Arabidopsis* seedlings in order to amplify the transcription products of TTL. Gel electrophoresis of the amplicons indicates the presence of two different species of transcript. Cloning and sequence analysis of the transcript forms revealed the effective presence of two different splice forms designated TTL^{1-} and TTL $^{2-}$ according to a recent proposed nomenclature [10]. These splicing variants correspond to transcript models present in the public databases (accession numbers NM_125207 and NM_001037017) and supported by EST and cDNA sequences, whereas a third putative transcript model (NM_001037016)

was not found in our analysis. TTL^{1-} encodes a 324 aminoacid protein while TTL^{2-} encodes a 311 aminoacid protein. In comparison to TTL^{1-}, the TTL^{2-} mRNA lacks nucleotides 883-921 of the pre-mRNA due to the usage of a downstream splice acceptor site within the third intron of the *TTL* gene (figure 2.2). Interestingly, the missing portion of the TTL coding sequence contains a non canonical peroxisome type 2 target signal (PTS2; RLx_5HL), located within the linker between the Urad and Urah domains.

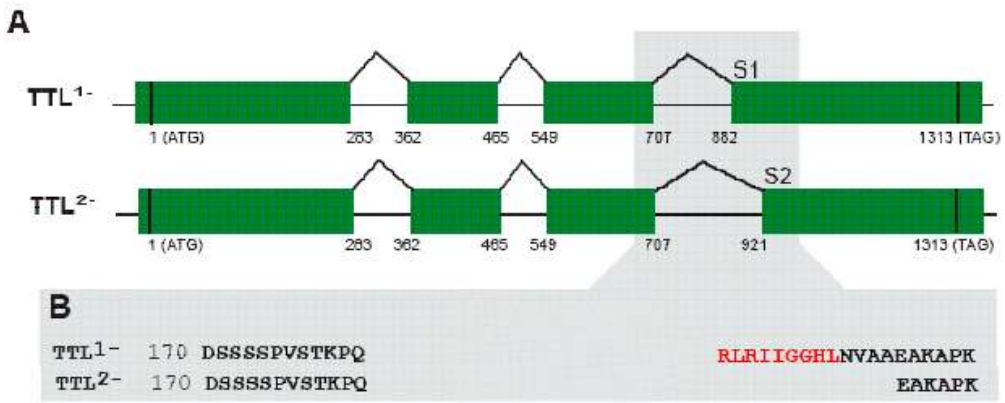

Figure 2.2 Differential splicing of TTL gene. (A) Schematic overview of the transcript variants of the *A. thaliana* TTL gene. The intron boundaries are numbered. (B) Sequence detail of the protein produced after the alternative splicing.

TTL splice variants have different intracellular localisation.

In order to clarify the sub-cellular localization of the two TTL splice variants previously identified, were created two C-terminal fusions of TTL^{1-} and TTL^{2-} with the green fluorescent protein (GFP). The fusion proteins were transiently expressed in *Arabidopsis* protoplasts or also co-expressed with markers for peroxisome or cytoplasm. A yellow fluorescent protein with a C-terminal Ser-Lys-Leu targeting signal (YFP-SKL) was used as a peroxisomal marker and an unmodified YFP as a cytosolic marker. Unlabeled samples were used to establish the levels and locations of the autofluorescence due to chloroplasts and single-labeled controls were used to assess bleed-through between fluorochromes. These procedures allowed selection of emission filter sets giving negligible cross-talk between fluorochromes in the different detection channels (figure 2.3).

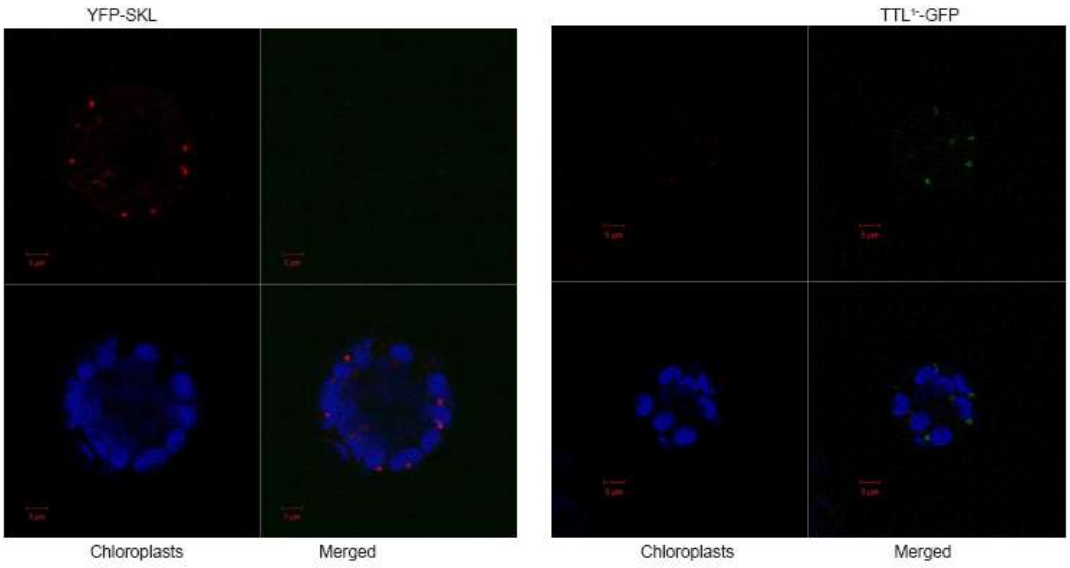

Figure 2.3 In vivo localisation of single-labeled proteins used to assess bleed-through between fluorochromes

Upon transient expression, TTL^{1-}-GFP localized to punctuated cellular structures overlapping with the structures labelled by the peroxisomal YFP, whereas TTL^{2-}-GFP co-localized with the cytosolic YFP (figure 2.4).

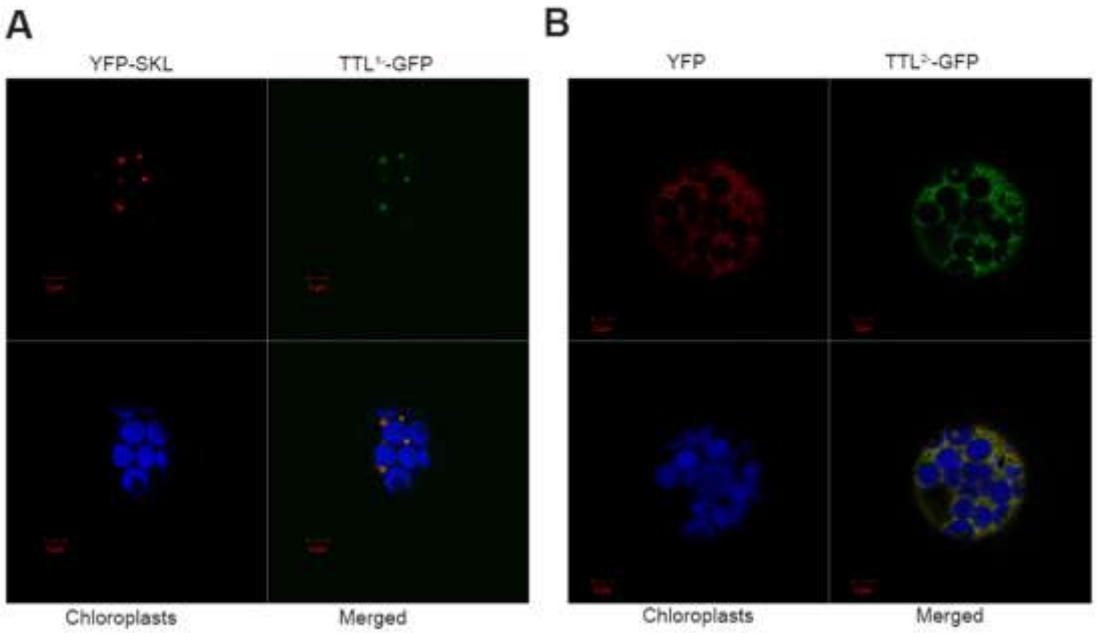

***Figure 2.4 In vivo* localisation of TTL^{1-} and TTL^{2-} splice variants**. Fluorescence in the range of 649-767 nm (chlorophylls), 490-510 nm (GFP), 542-596 nm (YFP) were monitored separately by confocal microscopy with a x100 objective lens. Chlorophyll, GFP fluorescence and YFP fluorescence are indicated by blue, green and red coloring, respectively.

Given the unusual internal position of the PTS2 signal of TTL^{1-}, to rule out the possibility that the TTL^{1-}-GFP was directed to peroxisome after a proteolytic cleavage exposing the PTS2 at the N terminus, was created the N-terminal GFP fusions of TTL^{1-}. The GFP-TTL^{1-} fusion protein exhibited the same punctuated localization as TTL^{1-}-GFP and YFP-SKL (figure 2.5).

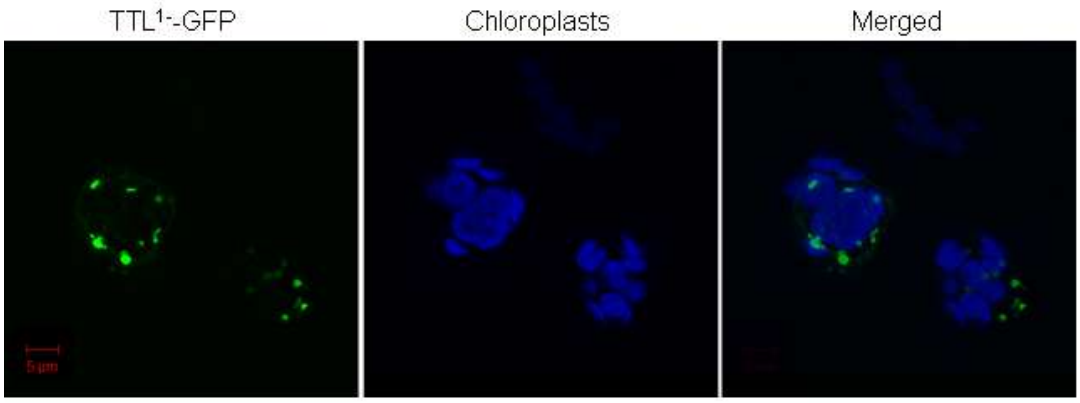

Figure 2.5 Fluorescence of N-terminal GFP fusion of TTL^{1-}

Here it is demonstrate that the internal PTS2 signal of TTL^{1-} can direct the TTL^{1-} protein at the peroxisomes, the sub-cellular compartment where ureide synthesis occurs. In the absence of the differentially spliced targeting signal, TTL^{2-} is incapable to enter the peroxisomes and the protein is thus retained in the cytosol. In a previous study TTL^{2-} was associated to the plasma membrane, in this study it was not possible to detect any differences between cytosolic YFP and TTL^{2-}GFP suggesting that previously observed membrane association [7] could not be detected with this transient expression system.

Biochemical identification of the Arabidopsis bi-functional S-allantoin synthase.

In order to evaluate their properties as a bi-functional enzyme in the pathway leading to the synthesis of S-allantoin, the TTL proteins were cloned, over-expressed and purified.
TTL^{1-} and TTL^{2-} were amplified and the PCR products were cloned in pET28-Cpo, a bacterial vector for the over-expression of histidine-tagged TTL. Following affinity chromatography, purified TTL were utilized for testing the activity in the conversion of HIU into allantoin.
Because the intermediates involved in the conversion of uric acid into allantoin are optically active compounds, the reactions can be followed by observing circular dichroism (CD) spectroscopy. The two intermediates, HIU and OHCU, can be distinguished by observing CD signals at 312 nm, where only HIU has appreciable ellipticity, and at 257 nm where only OHCU has appreciable ellipticity (Figure 2.6).

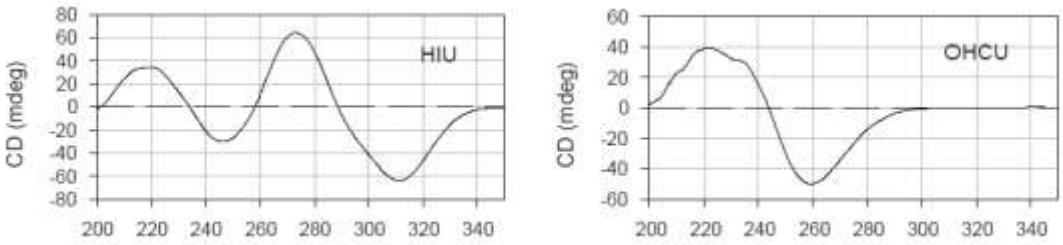

Figure 2.6 Approximate CD spectra of HIU and OHCU. HIU and OHCU, can be distinguished by observing CD signals at 312 nm, where only HIU has appreciable ellipticity, and at 257 nm where only OHCU has appreciable ellipticity

When only urate oxidase and uric acid are present in the reaction mixture, levorotatory HIU is initially produced as revealed by formation of negative peak around 312 nm. Spontaneous hydrolysis of HIU then produces levorotatory OHCU, as revealed by formation of a negative peak around 257 nm. Spontaneous decay of OHCU gives allantoin as a stable end product.
At millimolar substrate concentrations the urate oxidase reaction is complete after several hours and yields optically inactive RS-allantoin [1].

In the presence of Urah and Urad, instead, two enzymatic steps take place in the reaction mixture [2]: levorotatory HIU is hydrolysed to levorotatory OHCU by Urah and OHCU is steroselectively decarboxylated by Urad to give dextrotatory S-allantoin (Figure 2.7). Accumulation of S-allantoin in the reaction mixture and can be monitored due to its characteristic peaks around 220 and 242 nm.
When urate oxidase as well as purified *Arabidopsis* TTL were both added in the reaction mixture we observed the rapid decay of HIU and OHCU, and formation of optically active S-allantoin (figure 2.7).

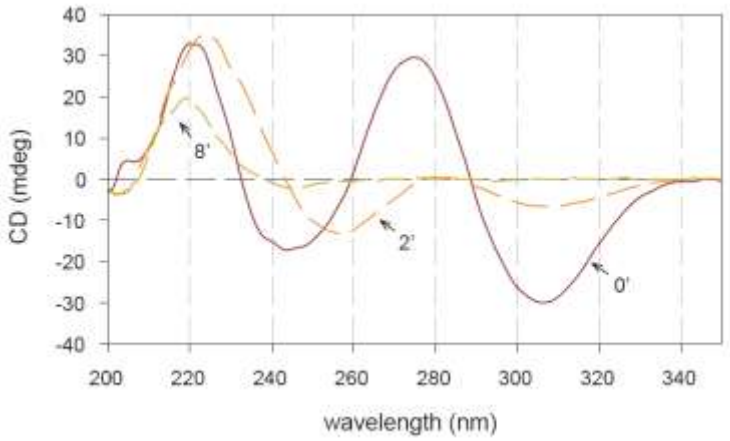

Figure 2.7 Time resolved CD spectra of the conversion of uric acid (0.1 mM in 100 mM potassium phosphate, pH 7.6) in the presence of urate oxidase and *A. thaliana* TTL (10 nM). Start time (0'): all the uric acid is converted into HIU by urate oxidase. After 2' HIU is almost entirely converted in OHCU. After 8' all the substrate is converted in S-allantoin.

This result proves that both TTL proteins have HIU hydrolase and OHCU decarboxylase activities and are able to catalyze the stereo-selective conversion of uric acid oxydation products into S-allantoin. Given the importance of this latter compound in ureide metabolism, and the evidence that allantoin is product in peroxisome it was proposed the name S-allantoin synthase for the plant TTL[1-] enzyme. Based on sequence comparison (see figure 2.1) is possible to conclude that the C-terminal domain of TTL catalyzes HIU hydrolysis, while the N-terminal domain of TTL catalyzes decarboxylation of OHCU to give S-allantoin.
The two enzymatic activities of TTL were separately monitored by observing time courses of the enzyme activity in the presence of HIU or OHCU as substrates (figure 2.8).

The velocity of the reaction was similar for the two substrates and it was proportional to the protein concentration (figure 2.8). After correction for the spontaneous decay rate of the substrates, a specific activity was calculated to be ~30 U/mg for HIU hydrolysis and ~26 U/mg for OHCU decarboxylation for TTL^{1-}. A comparable activity was detected for TTL^{2-}.

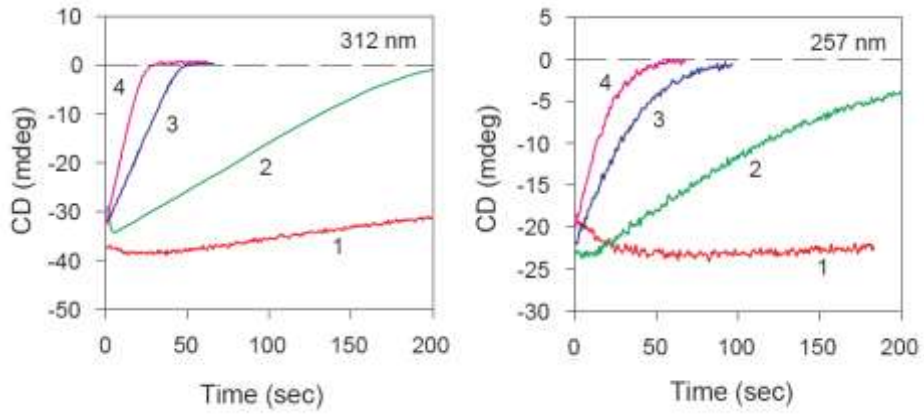

Figure 2.8 Time courses of the conversion of HIU (left panel; 312 nm) and OCHU (right panel; 257 nm) substrates in the presence of different TTL concentrations. 1) no enzyme; 2) 10 nM; 3) 100 nM; 4) 200 nM. Substrates were generated immediately before the reaction using uric acid (0.1 mM in 100 mM potassium phosphate, pH 7.6) and urate oxidase (to produce HIU) or urate oxidase plus zebrafish HIU hydrolase (to produce OHCU).

TTL^2 biological role.

Even though TTL^{2-} has S-allantoin synthase activity *in vitro*, this could hardly be the function of the protein *in vivo*. HIU is an unstable substrate that should be only produced in peroxisomes trough oxidation of urate by urate oxidase, a prototypical peroxisomal enzyme in eukaryotes. The cytosolic localisation of the TTL^{2-} splice variant, thus suggest a different function for the protein. Alternative splicing is thought to be a mechanism for increasing the functional and regulatory complexity of the plant proteome [11]. In this case alternative splicing could conciliate a role in the ureide pathway, with previous evidence suggesting a role in hormone signalling [7]. Although it was not possible to observe a localization in plasma membrane of the GFP fusion protein in our system, the presence of the protein in the cytosol would be compatible with the supposed interaction with a plasma membrane brassinosteroid receptor.

Quaternary structure of TTL^{1-}

The three-dimensional structure of HIU hydrolase has recently been determined by four independent groups for bacterial [12-14] and vertebrate [6] organisms. HIU hydrolase is a homotetramer and the active site is create by the joint of two homodimers.

OHCU decarboxylase is a homodimer in zebrafish [15] and the structure of part of the coding sequence (residues 1–161, 483 bp) encoding the *A.thaliana* bifunctional enzyme (Urad domain) [8] reveals that in this condition the *Arabidopsis* protein is a dimer too with one active site in each monomer. In order to investigate the quaternary structure of TTL^{1-} protein we decided to conduct a gel filtration analysis because the full-length protein was highly insoluble and the crystallisation very hard to obtain. After the gel filtration analysis, the protein was found in more fraction than expected (figure 2.9) indicating that in our condition the quaternary structure of the protein is unstable.

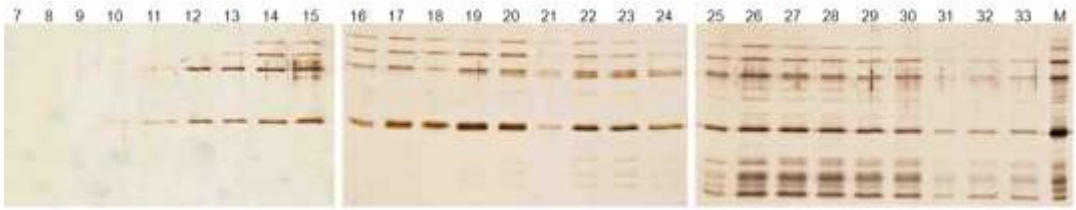

Figure 2.9 Elution pattern of TTL^{1-} in gel filtration experiment

Data obtained from atomic force microscopy (AFM) (figure 2.10) confirm that the TTL^{1-} have an heterogeneous composition and in this condition isn't possible to acquire information about the quaternary structure of this protein. However it is known from HIU hydrolase structure, that two active sites are formed at the interface between the two dimers that build up the protein tetramer [6, 13]. Therefore, a tetrameric organisation of TTL must be invoked to account for HIU hydrolase activity.

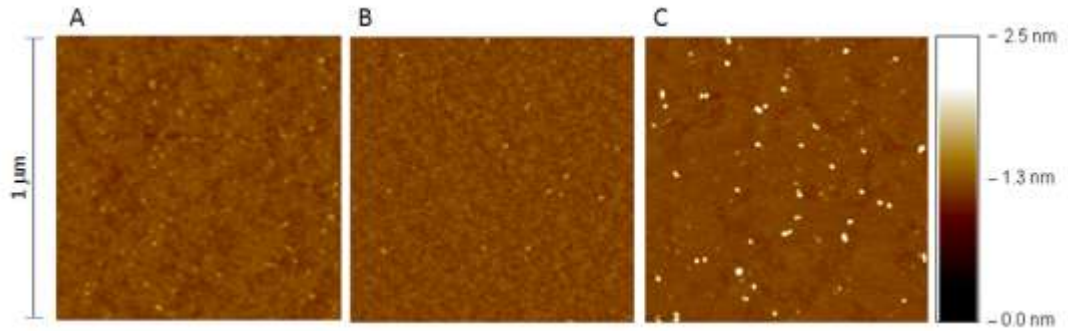

Figure 2.10 AFM images of (A) dimers of OHCU decarboxylase from zebrafish (40 kDa) (B) tetramers of HIU idrolase from zebrafish (53 kDa) (C) TTL^{1-} from *A. thaliana*. Contrary to the zebrafish proteins, the A*rabidopsis* protein shows an heterogeneous form.

Differential expression of TTL spliced transcripts in *Arabidopsis*.

To obtain insights in the expression of the TTL splice variants, the amounts of TTL^{1-} and TTL^{2-} in the whole *Arabidopsis* plant and in different tissues were quantified and compared by means of RT-PCR. Both splicing variants were detected in the samples analysed and the relative amount for the TTL^{1-} and TTL^{2-} forms did vary in the different organs tested (Figure 2.11). A similar amount of TTL^{1-} and TTL^{2-} transcripts is usually observed when is considered the ratio TTL^{2-}/TTL^{1-} (with a slight prevalence of TTL^{2-} transcripts). By contrast, floral buds appears to accumulate a much higher proportion (~5 fold) of the cytosolic (TTL^{2-}) form.

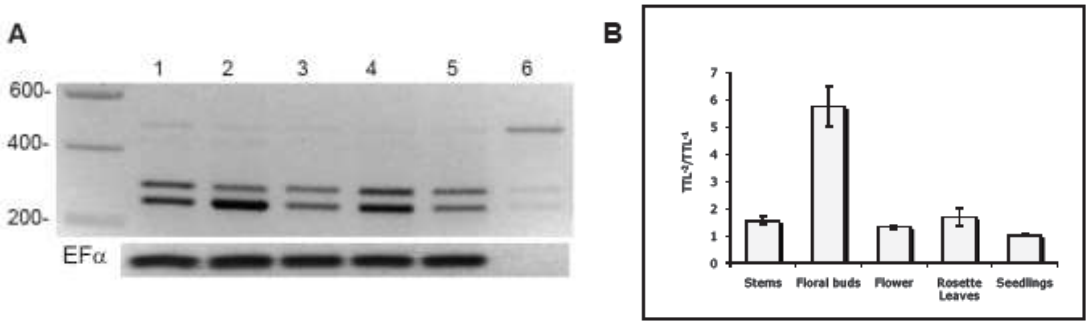

Figure 2.10 Differential expression of TTL^{1-} and TTL^{2-} splice variants. (A) RT-PCR analysis of TTL splice variants in different *A. thaliana* tissues. Total RNA was extracted from plant stem (line 1), floral buds (line 2), flower (line 3), rosette leaves (line 4), 3-day seedlings (line 5) . Control PCR reaction was conducted in the absence of reverse transcriptase (line 6). The Elongation Factor 1-α (EFα) was used as a reference gene. (B) Ratio of the amount of TTL^{2-} and TTL^{1-} transcripts. Data are presented with standard deviation values calculated from three independent biological replicates.

On the basis of the role of S-allantoin synthase in ureide biosynthesis it was also compared mRNA levels in plantlets grown on uric acid or allantoin as a nitrogen sources. With uric acid (5 mM) as the sole nitrogen source, seed germinated, but seedlings did not develop; to obtain growth beyond the cotyledon stage, low nitrogen (5 mM NH_4NO_3) had to be included in the growth media. In the presence of 5 mM allantoin, seedlings exhibited a phenotype with small, green leaves and strong root elongation as already reported [16]. The expectation was that higher levels of TTL^{1-} would be required, in order for the cell to utilise the nitrogen stored in uric acid, while lower levels of TTL^{1-} were expected in the presence of allantoin, the product of the reaction catalysed by the enzyme. In these experiments is not shown, however, substantial variation in the level of the two splice forms (figure

2.11 A), suggesting that the presence of exogenous ureides in the growth media does not affect expression of the gene in *A. thaliana*. It has been reported ureides are accumulated in *Arabidopsis* plant exposed to darkness, and that TTL is among the genes induced during dark stress [17]. The amount of TTL^{1-} and TTL^{2-} transcripts in seedlings placed in the dark for 2, 4, 6 days were analysed along with SRG1 mRNA, a well known dark-induced transcript (figure 2.11C). After the second day of dark treatment, TTL^{1-} transcripts increased slightly and become predominant over TTL^{2-} transcript (figure 2.11D).

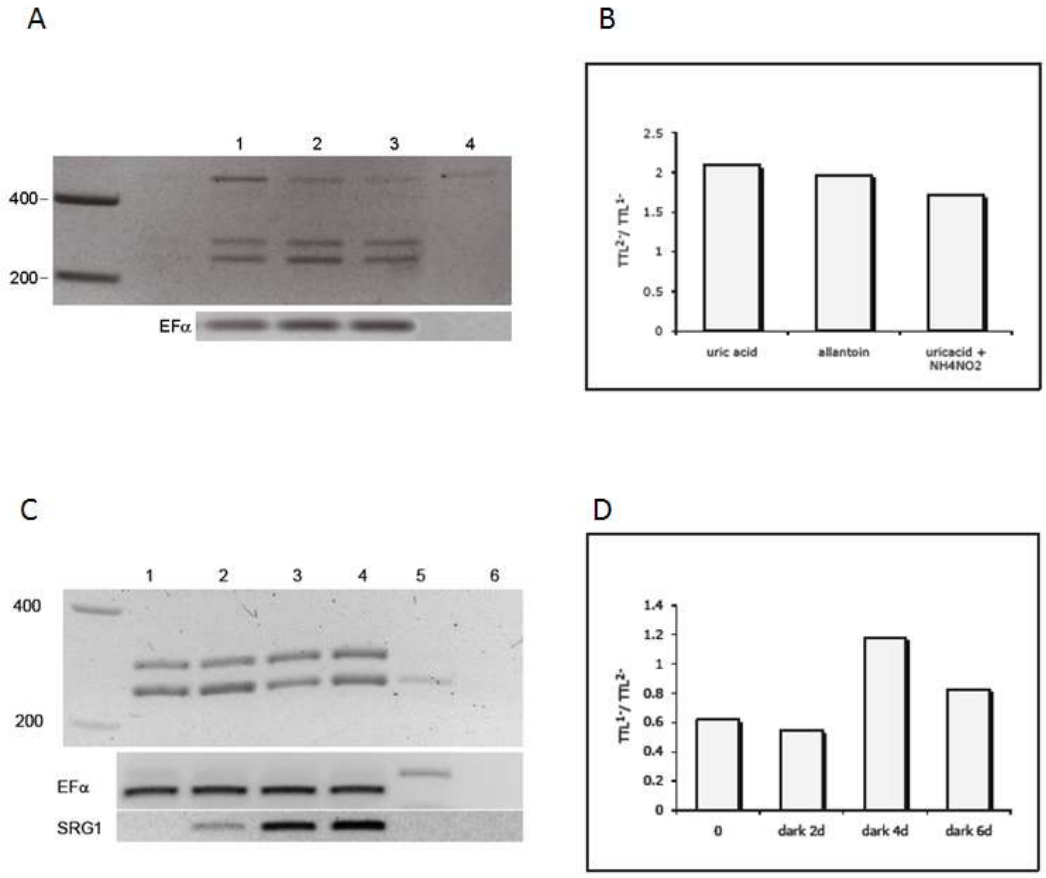

Figure 2.11 RT-PCR analysis of TTL splice variants in the presence of different nitrogen sources and in dark-treated plants. The reaction was performed cDNA generated from total RNA extracted from plants (A) grown on uric acid (line 1), allantoin (line 2), uric acid + NH_4^+ (line 3). Control PCR reaction was conducted in the absence of reverse transcriptase (line 4). The Elongation Factor 1-α (EF α) was used as a reference gene.
(C) RT-PCR on cDNA generated from total RNA extracted from plants not exposed to dark (line 1) or after two (line 2), four (line 3), and six (line 4) days of dark treatment. Control PCR reaction was conducted in the absence

of reverse transcriptase (line 5). The Elongation Factor 1-α (EF α) was used as a housekeeping reference gene. The Senescence Related Gene 1 (SRG1) was used as a dark-induced reference gene.

Evolutionary conservation of TTL alternative splicing in flowering plants.

EST analysis of TTL homolog sequences shows that alternative splicing occurs in other plants too. Conservation of alternative spliced forms in evolutionarily distant species is further evidence that the mechanism may play a biological significant role.

It was investigated by RT-PCR the existence of differently spliced transcripts in the monocot *Oryza sativa*. PCR primers were designed to amplify the linker region between the Urah and Urad domains. Gel electrophoresis of the amplification product showed the existence of two transcripts differing by about fifty nucleotides (figure 2.12A). Sequencing of the cloned PCR products and comparison with the *TTL* gene sequence revealed that in *O. sativa* two transcripts are produced through an alternative splicing which is very similar to that of *A. thaliana*. The intron undergoing alternative splicing is a phase 1 intron located between the two enzymatic domains, The splice donor sites are located at the same position as well as the first splice acceptor site (S1). The alternative acceptor site (S2) is located 39 nt. downstream in *A. thaliana* and 60 nt. downstream in *O. sativa*, and the two alternative transcripts differ only in a linker region between the two domains which encompasses the PTS2 sequence. Additional examples of alternative splicing are provided by EST analysis: different splice forms differing by the presence or the absence of the internal PTS2 are present in various plant species (figure 2.12B).

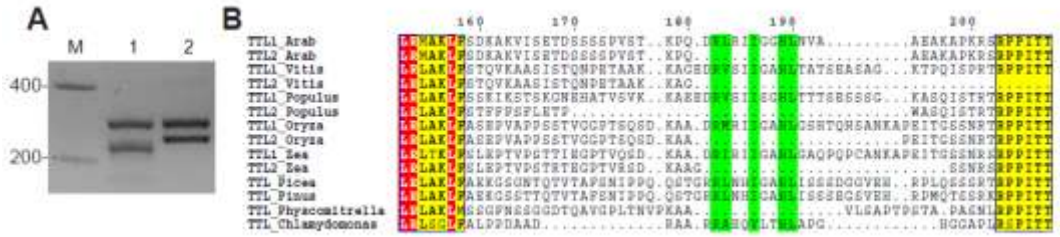

Figure 2.12 Conservation of TTL alternative splicing in plants. (A) RT-PCR analysis of TTL splice variants in *O. sativa* (line 1) and *A. thaliana* (line2); (B) Alignment of the linker region between urad and urah domain in various plants. Sequences were retrieved by homology searches in protein and EST databases and aligned with Clustalw. Conserved positions are shaded according with Espript [18]. The sequence motif corresponding to the PTS2 consensus is indicated in green.

A single TTL variant derives from intronless genes in the green alga *Chlamydomonas reinhardtii* and the moss *Physcomitrella patens*, with a recognizable PTS2 present in *C. reinhardtii* but not in *P patens.*

No evidence for alternative splicing were found in Gymonospermae transcripts, which were found always to encode proteins with internal PTS2. By contrast, evidence of alternative splicing is present in several Angiospermae, both in monocot and dicot species. In most cases examined, splice variant are generated by the use of an alternative splice acceptor site located between Urad and Urah domain, resulting in the inclusion or exclusion of the internal PTS2 in the coding sequence, and leaving the catalytic domains intact.

METHODS

Cloning, gene expression and protein purification. TTL transcripts were amplified from cDNA generated from total RNA extracted from *Arabidopsis* seedlings using the primers: 5'-ttcggtccgATGGCGATGGAGATCGGAG - 3' and 5' - ttcggaccgCTAGCTCCCACGGTATGTGGAGAAAG - 3'. All the primers bore 5'-tails such that the amplification products contained CpoI target sequences near to both ends. Amplicons were cloned into pGEM T- Easy vector (Promega). Plasmids were then inserted into XL1B E. coli cells (Stratagene) and the inserts were sequence-verified. The plasmids were subsequently treated with CpoI to extract the fragments corresponding to the amplified full-length cDNAs, ready for subcloning into the expression vector pET28- CpoI. This plasmid is a derivative of pET28 (Novagen) modified to present a single CpoI restriction site in the cloning region, downstream to a sequence encoding a hexa-histidine tag (Angelo Bolchi, unpublished). *E. coli* BL21 (DE3) condon plus cells (Stratagene) transformed with TTL^{1-}-pET28-CpoI or TTL^{2-}-pET28-CpoI constructs were incubated at 37°C in a M9 minimal medium until they reached the optical density of 0.6 at 600 nm. Expression was induced by adding 1mM IPTG and transferring the culture at 4°C for 3 days.

Cells from 250 ml of culture were lysed by sixty 30'' bursts of sonication in 100 ml of 50 mM sodium phosphate, 300 mM NaCl, 10% glycerol, 0.005% Tween 20, pH 7.5. Proteins were purified by TALON Metal Affinity Resin (Clontech) and eluted by adding 100 mM imidazole with a final yield of ~4 mg per liter of cell culture.

Biochemical assays. Enzymatic activity of TTL^{1-} TTL^{2-} splice variant were monitored by CD measurements carried out in a 10 mm pathlength cuvette with a Jasco J715 spectropolarimeter. The degradation of urate (0.1mM) in 1 ml of 0.1 M potassium phosphate pH 7.6 was monitored in the 200-350 nm range in presence of urate oxidase from Candida utilis (0.8 U, Sigma) and in presence or in absence of TTL^{1-} or TTL^{2-}. Single length measurements were carried out for HIUase activity at 312 nm and for OHCU decarboxylase activity at 257 nm in presence of 0,6 µg of zebrafish HIUase [6]. Activities of the bifunctional TTL protein were compared to the activities of zebrafish HIUase and OHCU decarboxylase [15] monitored by single length measurement in the same reaction conditions.

Plant Material and growth conditions. Standard *A. thaliana* ecotype Columbia-0 was obtained from the European Arabidopsis Stock Centre. Seed sterilization, germination and plate culture of seedlings were carried out following the protocols recommended by the Arabidopsis Biological Resource Center. Plants were grown in a greenhouse in 16-h light/8-h dark cycle at 25°C. Protoplast isolation was conducted on plants grown 3- 4 weeks on soil. Total RNA was isolated from plants grown 4 weeks on soil (plant tissues) or from plants grown three days on plates with Murashige and Skoog (MS) media (total seedlings). Growth on different nitrogen sources was conducted on MS media without nitrogen, supplemented with urate 5 mM, or urate 5 mM plus NH_4NO_3 5mM, or allantoin 5 mM. For dark treatment 4-week-old plants grown on soil were transferred to a dark room. Rosette leaves were collected after 2, 4 and 6 days of dark treatment.

In vivo targeting of fusion proteins. To generate the chimeric fusion constructs**,** TTL^{1-}-pET28CpoI and TTL^{2-}-pET28CpoI were amplified with PfuUltra polymerase (Stratagene) using primers: At5g58220+ 5' -taggatccaaaaATGGCGATGGAGATCGGA - 3, At5g58220- 5'-tgctcaccatGCTCCCACGGTATGTGGA -3', introducing a 5' BamHI site plus a plant ribosome binding site consensus , and a 3' GFP sequence (10 nt.). Primer At5g58220- eliminate the TAA stop codon from TTL^{1-} and TTL^{2-}, allowing the GFP fusion. GFP was amplified using primers: GFP+ 5'–taccgtgggagcATGGTGAGCAAGGGCGAG - 3' and GFP- 5'–ttgagctcTTACTTGTACAGCTCGTCC - 3', introducing a TTL sequence (12 nt.) at the 5'-end of GFP, and a 3' SacI site. A third PCR with primers At5g58220+ and GFP, using as template the GFP and TTL^{1-} or TTL^{2-} gave the fusion constructs TTL^{1-}-GFP and TTL^{2-} –GFP, which were cloned in pNEB193 following published protocols [19]. The ligated plasmids were then transformed into XL1B E. coli cells (Stratagene) and the inserts were sequence-verified. The plasmids were subsequently treated with BamHI and SacI and subcloned into the plant expression vector pPZPY122.

The YFP-SKL peroxisome marker was amplified by PCR with primers: 5'-ttggtaccaaaaATGGTGAGCAAGGGCGAG - 3' and 5' - ttctagatttacaattttgaCTTGTACAGCTCGTCC - 3', introducing a BamHI site plus a plant ribosome binding site at the 5'end, and a PTS1 sequence plus a KpnI site at the 3'-end. The YFP cytoplasm marker was amplified with primers: 5' –ttggtaccaaaaATGGTGAGCAAGGGCGAG - 3' and 5'- attctagaTTACTTGTACAGCTCGTCCATG, introducing a BamHI site plus a plant ribosome binding site at the 5'-end, and a XbaI site at the 3'-end. YFP and YFP-SKL were cloned in pART7 vector following published protocols [19] and the inserts were sequence-verified. The fusion constructs were introduced by polyethylene glycol–mediated transformation into *Arabidopsis* protoplasts prepared from plant leaves [20]. Transformed protoplasts were incubated in darkness at 23°C for 16-24 h before checking the fluorescence. Cells were mounted in custom-made chambers [21] and observed by confocal microscopy (x100 objective lens, 488 nm excitation) using a LSM 510 Meta scan head equipped with an Axiovert 200 M inverted microscope (Carl Zeiss, Jena, Germany).

RNA isolation and semiquantitative RT-PCR. Tissues for total RNA preparation were frozen in liquid nitrogen and pulverized using a pestle. The powdered tissues were transferred in buffer A containing: NaCl 0.6M, SDS 4%, EDTA 10 mM, Tris - HCl 100 mM pH8. Total RNA was isolated following a described miniprep procedure [22] except that phenol:chloroform (1:1) was used for extraction. RNA was recovered by precipitation in 4.4 M LiCl. Reverse transcription of 2 µg of total RNA was performed with Superscript III reverse transcriptase (Invitrogen) and an Oligo d-T primer in a 20µl-reaction. A 2-µl aliquot of the reaction mixture was used as a template for PCR amplification with TTL-specific primers designed to discriminate TTL^{1-} and TTL^{2-} transcripts (forward, 5'-GCTCTCCTGTTTCAACAAAACC - 3'; reverse, 5'- GGATTCAAAGCGTCAACCAAATC - 3'). All the reaction were normalized with the Elongation factor 1α (At5g60390) as housekeeping gene (forward, 5'- GGCTGATTGTCAGACCCGTGAGCAC -3'; reverse, 5'- GGAGTATTTGGGGGTGGTGGCATCCA

T - 3'). SRG1 (senescence related gene 1; At1g17020) was amplified using the following primers: forward 5'- AAGAGTGGGGATTTTTCCAGCTTGT -3' and reverse 5'- TGCCCAATCTAGTTTCTGAT CTTCTGA -3'. TTL transcripts from *Oryza sativa* were amplified using primers: forward: 5'-AGAACTGAAGATAACTGAACTGCG-3' and reverse 5'-GGTGTTGATGCATCCTTCCACAT-3'. PCR products were loaded on agarose 1,8% TBE gel and stained with ethidium bromide.

REFERENCES

1. Kahn, K. and P.A. Tipton, *Spectroscopic characterization of intermediates in the urate oxidase reaction.* Biochemistry, 1998. **37**(33): p. 11651-9.
2. Ramazzina, I., et al., *Completing the uric acid degradation pathway through phylogenetic comparison of whole genomes.* Nat Chem Biol, 2006. **2**(3): p. 144-8.
3. Sarma, A.D., et al., *Identification and purification of hydroxyisourate hydrolase, a novel ureide-metabolizing enzyme.* J Biol Chem, 1999. **274**(48): p. 33863-5.
4. Raychaudhuri, A. and P.A. Tipton, *Cloning and expression of the gene for soybean hydroxyisourate hydrolase. Localization and implications for function and mechanism.* Plant Physiol, 2002. **130**(4): p. 2061-8.
5. Lee, Y., et al., *Transthyretin-related proteins function to facilitate the hydrolysis of 5-hydroxyisourate, the end product of the uricase reaction.* FEBS Lett, 2005. **579**(21): p. 4769-74.
6. Zanotti, G., et al., *Structure of zebra fish HIUase: insights into evolution of an enzyme to a hormone transporter.* J Mol Biol, 2006. **363**(1): p. 1-9.
7. Nam, K.H. and J. Li, *The Arabidopsis transthyretin-like protein is a potential substrate of BRASSINOSTEROID-INSENSITIVE 1.* Plant Cell, 2004. **16**(9): p. 2406-17.
8. Kim, K., J. Park, and S. Rhee, *Structural and functional basis for (S)-allantoin formation in the ureide pathway.* J Biol Chem, 2007. **282**(32): p. 23457-64.
9. Reumann, S., et al., *Proteome analysis of Arabidopsis leaf peroxisomes reveals novel targeting peptides, metabolic pathways, and defense mechanisms.* Plant Cell, 2007. **19**(10): p. 3170-93.
10. Sammeth, M., S. Foissac, and R. Guigo, *A general definition and nomenclature for alternative splicing events.* PLoS Comput Biol, 2008. **4**(8): p. e1000147.
11. Reddy, A.S., *Alternative splicing of pre-messenger RNAs in plants in the genomic era.* Annu Rev Plant Biol, 2007. **58**: p. 267-94.
12. Hennebry, S.C., et al., *The crystal structure of the transthyretin-like protein from Salmonella dublin, a prokaryote 5-hydroxyisourate hydrolase.* J Mol Biol, 2006. **359**(5): p. 1389-99.
13. Jung, D.K., et al., *Structural and functional analysis of PucM, a hydrolase in the ureide pathway and a member of the transthyretin-related protein family.* Proc Natl Acad Sci U S A, 2006. **103**(26): p. 9790-5.
14. Lundberg, E., et al., *The transthyretin-related protein: structural investigation of a novel protein family.* J Struct Biol, 2006. **155**(3): p. 445-57.
15. Cendron, L., et al., *The structure of 2-oxo-4-hydroxy-4-carboxy-5-ureidoimidazoline decarboxylase provides insights into the mechanism of uric acid degradation.* J Biol Chem, 2007. **282**(25): p. 18182-9.
16. Desimone, M., et al., *A novel superfamily of transporters for allantoin and other oxo derivatives of nitrogen heterocyclic compounds in Arabidopsis.* Plant Cell, 2002. **14**(4): p. 847-56.
17. Brychkova, G., et al., *A critical role for ureides in dark and senescence-induced purine remobilization is unmasked in the Atxdh1 Arabidopsis mutant.* Plant J, 2008. **54**(3): p. 496-509.
18. Gouet, P., et al., *ESPript: analysis of multiple sequence alignments in PostScript.* Bioinformatics, 1999. **15**(4): p. 305-8.
19. Bolchi, A., S. Ottonello, and S. Petrucco, *A general one-step method for the cloning of PCR products.* Biotechnol Appl Biochem, 2005. **42**(Pt 3): p. 205-9.
20. Abel, S. and A. Theologis, *Transient transformation of Arabidopsis leaf protoplasts: a versatile experimental system to study gene expression.* Plant J, 1994. **5**(3): p. 421-7.
21. Gatti, R., Orlandini, G., Uggeri, J., Belletti, S., Galli, C., Raspanti, M., Scandroglio, R., and Guizzardi, S. (2008). Analysis of living cells grown on different titanium surfaces by time-lapse confocal microscopy. Micron 39, 137-143.
22. Sokolowsky, V., Kaldenhoff, R., Ricci, M., and Russo, V. (1990). Fast and reliable mini-prep RNA extraction from Neurospora crassa. Fungal Genet Newslett 37, 41–43.

Chapter 3

S-UREIDOGLYCINE AMIDOHYDROLASE

S-ureidoglycine aminohydrolase

ABSTRACT

In the ureide pathway, nitrogen is released as ammonia from allantoate through a series of reactions starting with allantoate amidohydrolase, a manganese-dependent enzyme found in plants (AAH) and bacteria (AllC). The true reaction product of allantoate amidohydrolase is S-ureidoglycine, a non-standard alpha-amino acid, and not ureidoglycolate. Ureidoglycine spontaneously decays into urea and glyoxylate *in vitro*, while living cells produce S-ureidoglycolate. Using gene proximity and logical genome analysis, we identified a candidate gene (*ylbA*) for S-ureidoglycine metabolism. The proteins encoded by *Escherichia coli* and *Arabidopsis thaliana* genes catalyze the Mn-dependent release of ammonia through hydrolysis of S-ureidoglycine yields S-ureidoglycolate. S-ureidoglycine amidohydrolase in plants is localized, like allantoate amidohydrolase, in the endoplasmic reticulum.

INTRODUCTION

Allantoin produced in peroxisomes is translocated in the endoplasmic reticulum and hydrolyzed by allantoinase to produce allantoate [1]. The breakdown of allantoate yields usable nitrogen for subsequent anabolic reactions. In general, allantoate can be hydrolyzed by two different enzymes, allantoate amidohydrolase (EC 3.5.3.9) and allantoicase (EC 3.5.3.4). Allantoate amidohydrolase releases NH_3 and CO_2 directly from allantoate, whereas allantoicase produces urea, which can then be converted to NH_3 and CO_2 by the nickel-dependent enzyme urease (EC 3.5.1.5) [2] (figure 3.1).

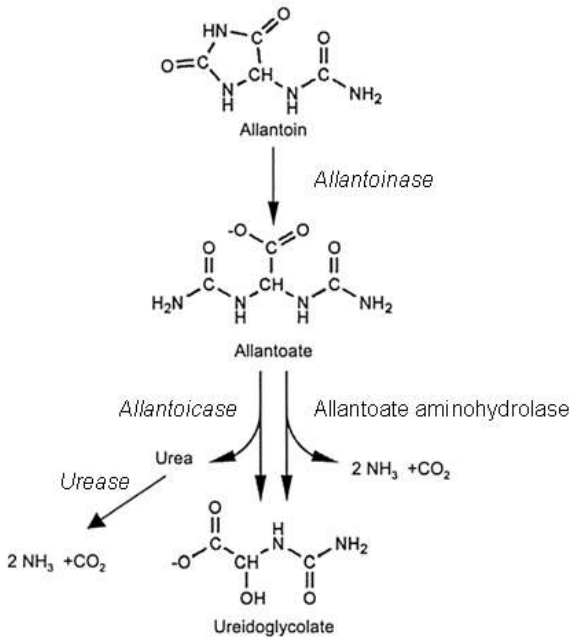

Figure 3.1 Degradation of allantoin to ureidoglycolate.
The intermediate allantoate can be hydrolyzed by two different enzymes: allantoicase and allantoate amidohydrolase. (Adapted from Todd et al.) [2].

Allantoicase is typically found in animals, fungi and several bacteria, while some other bacteria and all plants use allantoate amidohydrolase [3, 4]. Allantoate amidohydrolase from *E. coli* (AllC) has been extensively studied: the crystal structure of the protein in complex with the substrate has been resolved [5], it's known that AllC is a manganese-dependent protein [4, 6] and in plants this enzyme is located in the endoplasmic reticulum [4]. Paradoxically, however, a fundamental question about this enzyme has never been fully answered: what reaction does it catalyze?

Early studies have established that the AllC reaction produces two moles of ammonia, one mole of carbon dioxide and one mole of ureidoglycolate as a stable end product per mole of allantoate.

Accumulation of an intermediate during the reaction was assumed because of the formation of glycine through a side transamination reaction in the presence of glyoxylate [6]. The identification of ureidoglycine as intermediate is based on this observation and on similarities with other amidohydrolases rather than on direct evidence. Moreover, it is unclear if the ureidoglycine intermediate is converted to ureidoglycolate by the action of AllC [6, 7] or by the action of a distinct, as yet unidentified, enzyme [5, 8, 9]. These two possibilities are alternatively accounted for by the major databases of biological reactions.

RESULTS AND DISCUSSION

Identification of ylbA as a candidate for S-ureidoglycine aminohydrolase function

Even if the hydrolysis of ureidoglycine is spontaneous *in vitro*, in nature there should be an enzyme to catalyze this reaction. First, the spontaneous release of ammonia from ureidoglycine appears to be too slow to sustain an efficient flux of nitrogen through the ureide pathway; second, in living cells, the reaction is known to produce a single enantiomer of ureidoglycolate, S-ureidoglycolate [10], while the spontaneous hydrolysis of ureidoglycine would produce a racemic mixture. In fact, by monitoring the AllC reaction by CD spectroscopy one does not observe formation of optically active ureidoglycolate as a final product. It was identified a canditate for ureidoglycine amidohydrolase searching for uncharacterized genes present in bacterial genomic clusters containing allantoate amidohydrolase [11]. As a further condition, it was necessary that orthologous genes be present in organisms containing allantoate amidohydrolase (both prokaryotes and eukaryotes) and absent in organisms containing allantoicase (these organisms are not expected to form ureidoglycine). The search identified the *E. coli ylbA* gene [12] as a candidate ureidoglycine aminohydrolase. The *ylbA* gene is immediately downstream from the *allC* gene in the *E. coli* genome (figure 3.2) and is present in several purine degradation clusters along with *allC*.

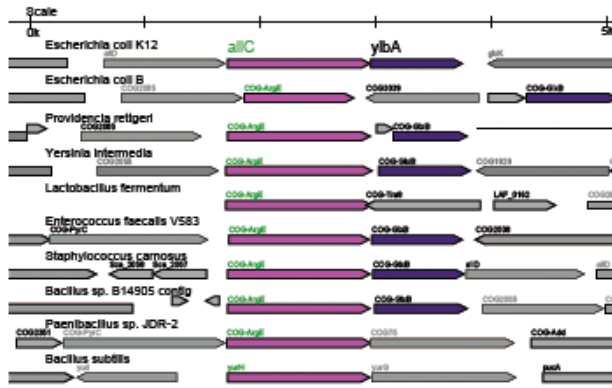

Figure 3.2 Identification of YlbA as a candidate S-ureidoglycine hydrolase. Comparison of the genetic context of the allC gene (magenta) in *E. coli* genome and other bacteria showing the frequent association with the ylbA gene (blue) [11].

Homology searches and phylogenetic analysis indicate that genes closely related to *ylbA* are present in plants and green algae (which possess allantoate amidohydrolase), but not in metazoa and the majority of fungi (which possess allantoicase). A more distant clade of *ylbA*-related genes is found in organisms (bacteria and some fungi) devoid of both allantoicase and allantoate amidohydrolase.

Three-dimensional structures are available for the *E. coli* YlbA proteins (PDB code 1RC6) and for other three bacterial related proteins; all these structures have been solved via structural genomics and correspond to uncharacterized proteins.

Expression and purification of recombinant *E. coli* YlbA allow to confirm, throgh a coupled assay with glutamate dehydrogenase, that this protein has ureidoglycine aminohydrolase activity [11].

The *ylbA* gene of *E. coli* of encodes a protein of 261 amino acids. The homologous gene of *A. thaliana* ($p<10^{-28}$) encodes a protein of 298 amino acids with 28% amino acid identity (At YlbA). Difference in protein length is determined by an extra N-terminal segment which is present only in plant sequences (figure 3.3), and it is predicted that it contains a cleavable signal peptide.

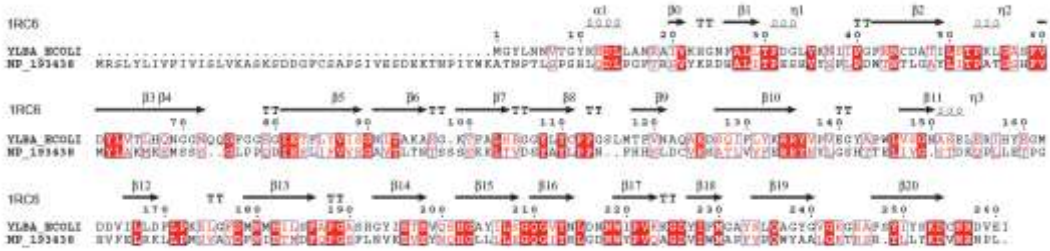

Figure 3.3 Alignments of *E. coli* YlbA with the homologous protein from *A. thaliana*.
Conserved positions are shaded according with the similarity criteria of Espript [13]; secondary structure elements derived from the 3D coordinates of *E. coli* YlbA (1RC6) are drawn above the alignment.

Arabidopsis YlbA (AtYlbA) is a ureidoglycine aminohydrolase

Full-length AtYlbA and a truncated variant (ΔAtYlbA) starting at Pro51, lacking a putative signal peptide and a short plant-specific sequence (see figure 3.3) were cloned and purified in *E. coli* near homogeneity by metal affinity chromatography. The protein corresponding to the full-length plant sequence was found to be largely insoluble, while the truncated variant was found to be soluble and was used for biochemical characterization.

AllC reaction produces two moles of ammonia per mole of allantoic acid, the former is produced in few minutes, whereas the latter is produced in hours (figure 3.5 A). The last release of ammonia is attributable to the spontaneous degradation of ureidoglycine rather than an enzymatic activity.

By supplementing the AllC reaction mixture with the recombinant YlbA protein we observed the rapid release of two moles of ammonia per mole of allantoic acid (Figure 3.5 A); there were no release of ammonia or urea, however, if AllC was omitted from the reaction mixture (figure 3.5 A), suggesting that the YlbA uses the AllC reaction product, but not allantoic acid, as substrate. In fact when the YlbA protein was added after completing the first step of the AllC reaction, it caused the rapid release of a second mole of ammonia (Figure 3.5 B).

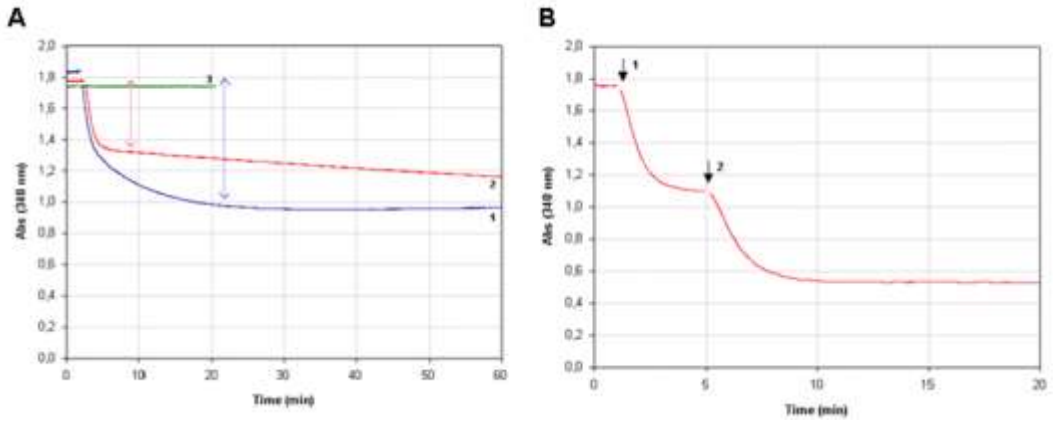

Figure 3.5 Time courses of ammonia release using a coupled assay with glutamate dehydrogenase.
(A) Time course of ammonia release by the AllC reaction monitored spectrophotometrically using a coupled assay with glutamate dehydrogenase. The reaction was initiate by the addition of 0.075 mM allantoate to a solution containing 0.13 µM AllC and 0.13 µM YlbA (1) or 0.13 µM AllC but not YlbA (2) or 0.13 µM YlbA but not AllC (3). (B) Time courses of ammonia release from allantoate (0.5mM), catalyzed by the successive additions of AllC and YlbA (2)

AllC and YlbA produce optically active ureidoglycine and ureidoglycolate.

Allantoate is a prochiral molecule in which each carbamoyl group is attached to a non standard amino acid (ureidoglycine). The pro-R carbamoyl is attached to an ureidoglycine moiety in an S-configuration while the Pro-S carbamoyl is attached to an ureidoglycine moiety in the R-configuration. Hydrolysis of a carbamoyl group is thus expected to produce optically active ureidoglycine, and a transient optically active compound with a spectrum similar to that of L-amino acids was observed by monitoring the reaction with CD spectroscopy (figure 3.6 A). The reaction product of allantoate in the presence of AllC and YlbA was found to be optically active, with a CD spectrum (Figure 3.6 B) matching a spectrum previously attributed to S-ureidoglycolate [10].

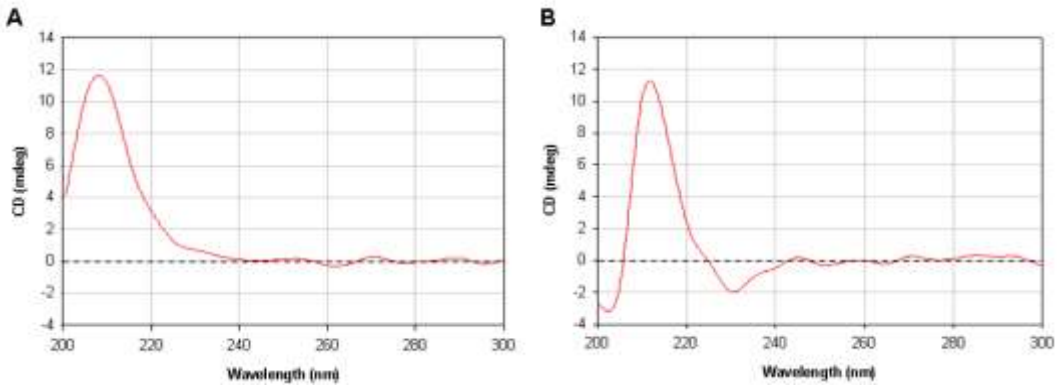

Figure (3.6) CD spectra of the optically active products obtained from allantoate in presence of AllC (a) or both AllC and AtYlbA (b).

ylbA encodes a Mn-dependent S-ureidoglycine aminohydrolase

Allantoate amidohydrolase from various sources is reported to be a Mn-dependent enzyme. To obtain maximum activity, the manganese ion was typically included in the AllC reaction mixture. However, freshly purified AllC preparations were catalytically active (albeit at a lower rate) even without the addition of metals, allowing the metal dependency of YlbA to be determined. In the absence of added metals, YlbA was found to be inactive. The activity could be completely restored by the addition of $Mn2^{+}$, and partially restored by the addition of Co_2+ or Zn_2^{+}; all the other divalent metals examined (Cu_2^{+}, Ca_2^{+}, Ni_2^{+}, Mg_2^{+}) were ineffective (figure 3.7).

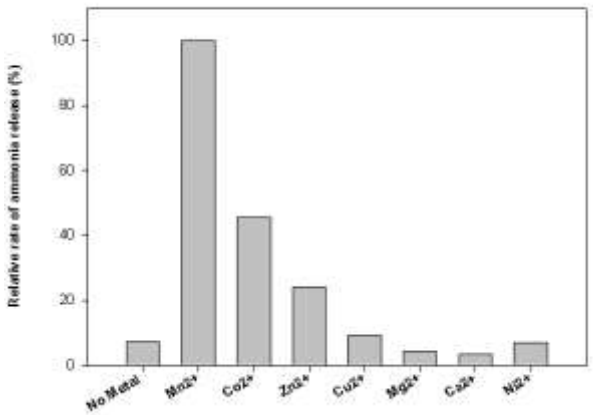

Figure 3.7 Relative rates of ammonia release by the YlbA-catalyzed reaction in presence of various divalent metals.

S-ureidoglycine hydrolase is a Mn dependent enzyme. The hydrolase activity is parzially restored by Co^{2+}. A light enzymatic activity is monitored in presence of Zn^{2+}.

Effect of Asparagine on YlbA

Purified AllC is inhibited by L-Asn and L-Asp and barely by D-Asn [4]. L-Asn resembles allantoate or ureidoglycolate and may rather function as a competitive inhibitor. The inhibitory effect of L-Asn can be suppressed by increasing substrate concentrations consistent with a competitive or mixed mechanism of inhibition [4].

In order to understand if YlbA activity is inhibited by L-Asn and/ or D-Asn we decided to test the protein with the same coupled assay used to determine the YlbA function in presence of 10 mM L-Asn or D-Asn (figure 3.8).

YlbA is inhibited by L-Asn at the same way of AllC; the inhibition of YlbA by D-Asn is more marked on YlbA activity rather than on AllC activity.

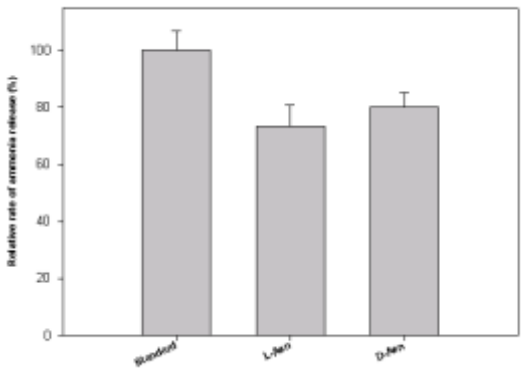

Figure 3.8 Inhibition of AtYlbA activity by asparagine.

YlbA is partially inhibited by L-Asn

AtYlbA modelling

The structure of AtYlbA has not been resolved, however, is possible to obtain a model searching for a template among the protein with resolved structure present in Protein Data Bank (PDB). The best sequence that can be used for modelling AtYlbA is a related protein from *Deinococcus radiodurans* (1SFN) As AtYlbA this protein has unknown function**.** The reconstructed structure shows two cupine domains; each cupin domainis made up of a small barrel (*cupa* in Latin) featuring two antiparallel β-sheets (figure3.9 A). The 3D structure reveals strong structural similarities between the N- and C-terminal halves of the protein, indicating that the bi-domain structure of AtYlbA originated from an ancestral duplication of a single cupin domain (figure 3.9 B)

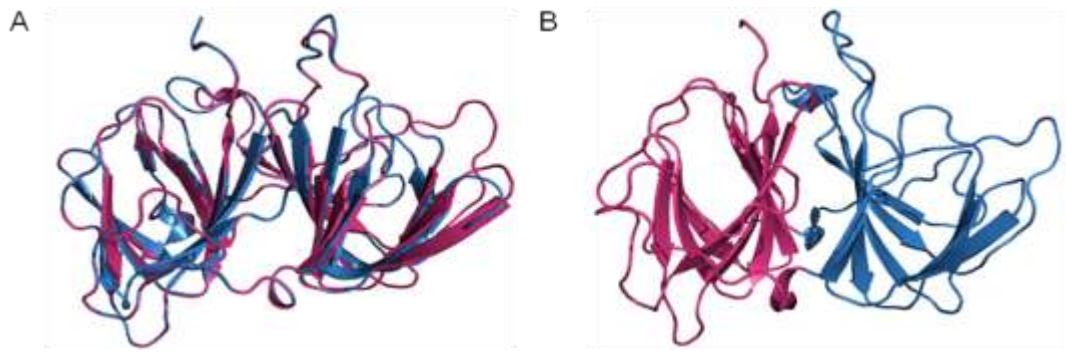

Figure 3.9 3D reconstruction of AtYlba. A) Overlapping of AtYlbA model (magenta) with the *Deinococcus radiodurans* related protein used as a template (blue) B) Cartoon sketch of the AtYlbA structure, highlighting the secondary structural elements and the bi-domain structure, with the N-terminal half (aa 1—149) in blue and the C-terminal half (aa 150—298) in magenta. b)

The presence of a cupin domain is found in several proteins classified in the cupin superfamily, functionally one of the most diverse seen thus far [14]. It comprises 20 families with members that perform diverse functions ranging from enzymatic to non enzymatic functions. AtYlbA is the prototypic member of a family that encompasses proteins whose function is unknown [15]. Structural similarities, however, reveal an evolutionary relationship between AtYlbA and proteins whose function is known. Interestingly, among the proteins of the cupin superfamily there are several Mn-dependent enzymes, such as ureidoglycolate hydrolase [16] (another enzyme of the purine catabolic pathway), oxalate oxidase, and oxalate decarboxylase. In most bicupins, an enzymatic activity is associated with only one of the two domains. Active domains usually have a metal-binding site (usually for Mn, Fe, or Zn) localized at the mouth of the barrel. Thus, structural alignment with known metal-binding cupins can identify residues involved in metal coordination [15]. The comparison of N-

and C-terminal domains of AtYlbA proteins with the Mn-binding domain of oxalate decarboxylase suggests the existence of a metal-binding site in domain II of AtYlbA. Unlike domain I, in which residues involved in metal coordination are replaced by not conserved hydrophobic residues, domain II shows the presence of potential metal-binding residues that are strictly conserved in the YlbA family. Although the configuration of potential metal-binding residues in the domain II of AtYlbA (His, Glu, His, Gln) differs from the canonical configuration of cupins (His, His, Glu His), the 3D superposition shows conservation of the geometry of the metal binding site.

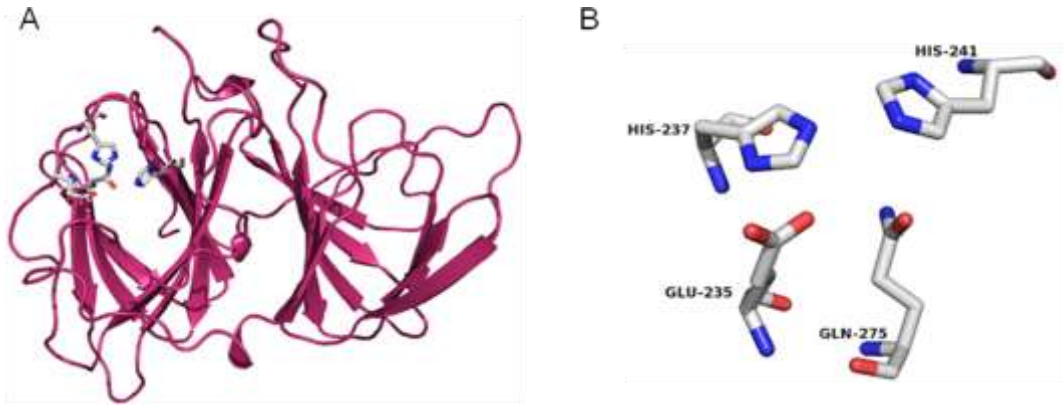

Figure 3.10 Hypothetical metal binding site of AtYlba. A) Metal binding site is positioned at the mouth of the barrel. B) Aminoacids involved in metal coordination.

Sub-cellular localization of plant S-ureidoglycine amidohydrolase.

In plants, allantoate amidohydrolase is localized in the endoplasmic reticulum (ER) [4]. The presence of S-ureidoglycine amidohydrolase in the same compartment where the unstable ureidoglycine is formed would make biological sense. Plant YlbA sequences have an extra N-terminal segment of ~40 aminoacids which, it has been predicted, contains a signal for the co- translational insertion of the protein in the ER (see Figure 3.3). The *Arabidopsis* as well as other plant sequences do not contain the known signature for ER retention (K/HDEL).

However, the presence of such a signal is not an absolute requirement for ER proteins [17]

In order to demonstrate the sub-cellular localization of S-ureidoglycine amidohydrolase, we constructed C-terminal fusions of full length *Arabidopsis* AtYlbA sequence with the yellow fluorescent protein (AtYlbA-YFP). The fusion protein was transiently expressed in *Arabidopsis* protoplast or also co-expressed with a green fluorescent protein fused with a signal peptide and an ER retention signal (GFP-HDEL) used as a marker for the ER. Upon transient expression, AtYlbA-YFP localized to cellular structures with the typical shape of the ER. The co-localization of AtYlbA-YFP and GFP-HDEL fusion proteins further supports an ER localization for the plant enzyme (figure 3.1). We

concluded from confocal microscopy studies that in plant cell, S-ureidolgycine amidohydrolase is localized in the same subcellular structure where S-ureidoglycine is formed.

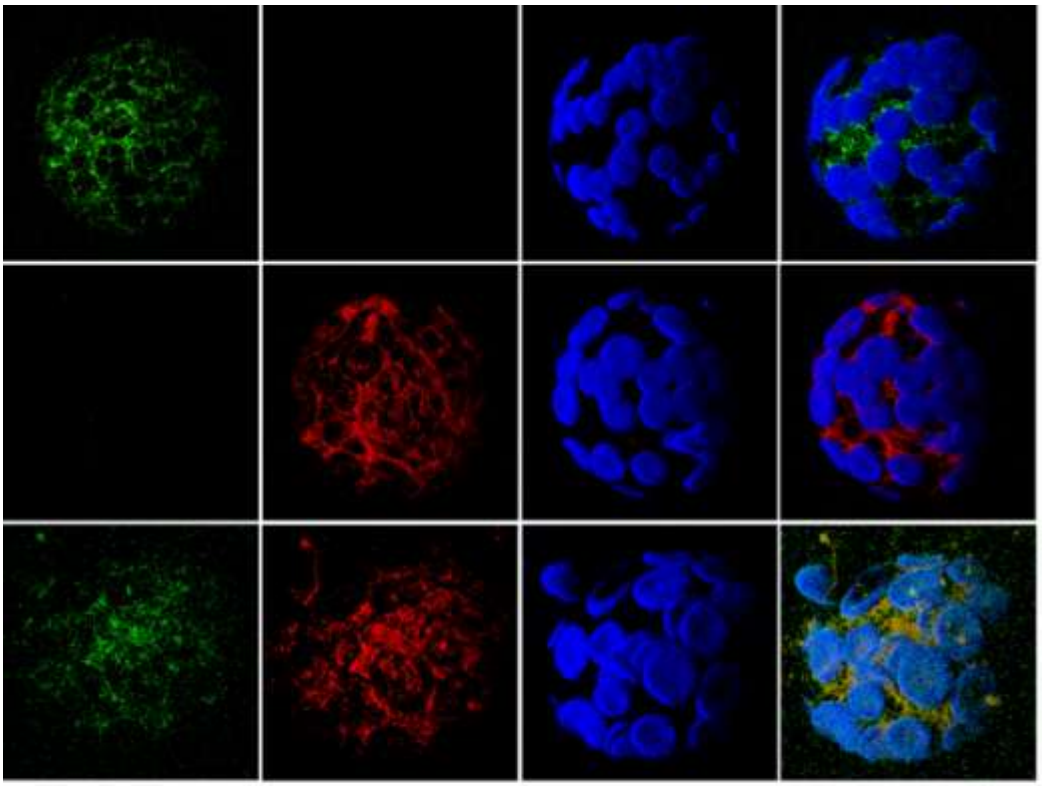

Figure 3.11 Subcellular localization of plant ureidoglicine amidoidrolase. 3D reconstruction of optical section of plant cells transformed with AtYlbA-YFP (red), GFP-HDEL (green) or both. Fluorescence in the range of 649-767 nm (chlorophylls), 490-510 nm (GFP), 542-596 nm (YFP) were monitored separately by confocal microscopy with a x100 objective lens.

METHODS

Cloning and production of recombinant proteins

Clones encoding full-length histidine-tagged AllC was obtained from the ASKA library [18]. Clones were verified by sequencing using primers based on the pCA24N vector. Amplicons encoding the full-length YlbA protein from *A. thaliana* (YlbA) were obtained by PCR amplification of total plant cDNA with the following primers: forward 5'-ATCGGTCCGGCAAAAATGCGATCACTTTAC-3' and reverse 5'- ATCGGACCGCTTTGATCACAATGGATTTCG-3'. Amplicons encoding a protein lacking the signal peptide and a plant-specific N-terminal sequence, starting from amino acid 51 of the *A. thaliana* YlbA (ΔYlbA) were obtained using a different forward primer (5'-ATCGGTCGGATGCCTTCACACCTCCAAGACTTG -3'). YlbA amplicons were cloned into pGEM-T Easy vector (Promega) and subcloned into the expression vector pET28-CpoI (A. Bolchi, unpublished). ΔYlbA amplicons were cloned directly into the expression vector pET28-SnaB1 (A. Bolchi, unpublished) using a one-step cloning procedure [19]. The ligated plasmid was then transformed into BL21 (DE3)-RIL *E. coli* cells (Stratagene) and the inserts were sequence verified. Transformed cells were grown at 37°C in LB medium and gene expression was induced at an optical density at 600 nm of 0.3 (AllC) or 0.6 (AtYlbA, ΔAtYlbA) using 0.5 (AllC) or 1 mM (AtYlbA, ΔAtYlbA) IPTG; after 48 h at 15 °C (AllC) or 24 h at 22 °C (AtYlbA, ΔAtYlbA) the cells were resuspended in lysis buffer (50 mM sodium phosphate, 0.3 M NaCl, 10% glicerol, 1 μM pepstatin, 1 μM leupeptin, 100 μM PMSF, 2 ml/ml lysozyme, pH 8) with (AllC) or without (AtYlbA, ΔAtYlbA) 1 mM β-mercaptoethanol, and incubated on ice for 30 min. Cells were lysed by four 15-second bursts of sonication and the crude cell extract was concentrated by ultrafiltration in an Amicon cell (YM-10 membrane, Millipore). Proteins were purified by affinity chromatography (Talon, Clontech) and assessed by SDS-PAGE analysis. Loaded columns were washed with buffer 50 mM Tris-HCl pH 7.0, 5% glycerol, 0.2 M NaCl and proteins were eluted with 50 mM (AllC) or 100 mM (AtYlbA) imidazole. AllC was conserved at 4 °C in the presence of 1 mM EDTA. This condition ensured a better, though not complete, stability of the enzymatic activity. AtYlbA was conserved at -20 °C in the elution buffer. In these conditions, the enzymatic activity was stable for several months.

Biochemical assays

Ammonia release by the AllC reaction was determined spectrophotometrically using a coupled assay with glutamate dehydrogenase (GDH) [6, 9]. The typical incubation mixture consisted of 1 ml of 0.2 M Tris-HCl buffer, pH 8.5, with 0.3 mM NADPH, 2.5 mM α-ketoglutarate, 4.12 units of GDH from *Proteus sp* (Sigma), 100 μM MnCl2, and 6 μg AllC. The reaction was initiated by the addition of allantoic acid (0.15 mM) and the decrease in absorbance at 340 nm due to the oxidation of NADPH was recorded. The effect of metal ions on the enzyme activity was determined by preincubating the enzyme with 10-fold to 1000-fold excess metal ions (Zn^{2+}, Co^{2+}, Cu^{2+}, Ca^{2+}, Ni^{2+}, Mn^{2+}, Mg^{2+}) in 0.2 M Tris-HCl, pH 8.5. Ammonia release by the YlbA reaction was determined using the same coupled

assay described above, in the absence or in the presence of AllC. Recombinant YlbA (6 µg) was added to the initial reaction mixture or after the fast phase of the AllC reaction. The effect of metal ions on the activity of YlbA was determined by excluding Mn2+ from the initial reaction mixture and by adding YlbA plus 100 µM metal ions (Zn^{2+}, Co^{2+}, Cu^{2+}, Ca^{2+}, Ni^{2+}, Mn^{2+}, Mg^{2+}) after the first phase of the AllC reaction.

Formation of optically active compounds in the reactions catalyzed by AllC and YlbA was monitored by CD measurements carried out in a 10 mm pathlength cuvette with a Jasco J-715 spectropolarimeter. The degradation of allantoic acid (700 µM) in 1 ml of 20 mM potassium phosphate, 100 µM $MnCl_2$, pH 7.6, was monitored in the 200-300 nm range in presence of *E. coli* AllC (20 µg) and in the presence or in the absence of *A. thaliana* YlbA (30 µg). Ureidoglycolate has a CD signal in a region of the spectrum where absorption by other compounds of the reaction mixture interferes with the measurements. CD signals could be obtained with appropriate reactant and buffer concentrations and by lowering the imidazole content of protein solutions.

In vivo localization of fluorescent proteins

To generate chimeric fusion construct of YlbA with the Yellow Fluorescent Protein (YFP), a pGEM plasmid containing the full-length plant YlbA sequence was amplified using primers forward 5'-ATCGGTCCGGCAAAAATGCGATCACTTTAC -3', and reverse 5'-TGCTCACCATCAATGGATTTC GATTCACAT -3', introducing a plant ribosome binding site at the 5' of the gene and a 5' YFP sequence (10 nt) at the 3' of the YLBA sequence. The reverse primer eliminates the TAA stop codon from YlbA, allowing YFP fusion. YFP was amplified using primers forward 5'-TCGAAATCCATTGATGGTGAGCAAGGGCGAG -3' and YFP reverse 5'- ATTCTAGATTACTTGT ACAGCTCGTCCATG -3' introducing a 3' YlbA sequence (13 nt) at the 5' of YFP and a 3' *Xba1* site. A third PCR with primers YLBA forward and YFP reverse, using as template the YLBA and YFP amplicons, gave the fusion construct YlbA-YFP which was cloned in pBluescript II KS/SK (+) following a published protocol [19]. The ligated plasmid was then transformed into XL1B *E .coli* cells (Stratagene) and the insert was sequence verified. The plasmid was subsequently treated with *EcoR1* and *Xba1* and sub-cloned into the plant expression vector pART7. The construct GFP-HDEL-pVKH18en6 was a kind gift from Janet Evins. The fusion constructs were introduced by polyethylene glycol-mediated transformation into protoplasts prepared from plant leaves [20]. Standard *Arabidopsis thaliana* ecotype Columbia-0 (European *Arabidopsis* Stock Centre) plants were grown 3-4 weeks on soil in 16-h light/8-h dark cycle at 25 °C. Transformed protoplasts were incubated in darkness at 23 °C for 16-24 h before checking the fluorescence. Cells were mounted in custom-made chambers and observed by confocal microscopy (x100 objective lens, 488 nm excitation) using a LSM 510 Meta scan head equipped with an Axiovert 200 M inverted microscope (Carl Zeiss, Jena, Germany). Unlabelled samples were used to establish the levels and locations of the autofluorescence due to plastids and single-label controls were used to assess bleed-through between fluorochromes, allowing the selection of emission filter sets giving negligible cross-talk

between fluorochromes with partially overlapping emission spectra. For 3D reconstructions, stacks of digital images were processed with the Axiovision software (Carl Zeiss, Jena, Germany) by applying the "shadow" algorithm.

REFERENCES

1. Hanks, J.F., N.E. Tolbert, and K.R. Schubert, *Localization of Enzymes of Ureide Biosynthesis in Peroxisomes and Microsomes of Nodules.* Plant Physiol, 1981. **68**(1): p. 65-69.
2. Todd, C.D. and J.C. Polacco, *Soybean cultivars 'Williams 82' and 'Maple Arrow' produce both urea and ammonia during ureide degradation.* J Exp Bot, 2004. **55**(398): p. 867-77.
3. Todd, C.D. and J.C. Polacco, *AtAAH encodes a protein with allantoate amidohydrolase activity from Arabidopsis thaliana.* Planta, 2006. **223**(5): p. 1108-13.
4. Werner, A.K., et al., *Identification, biochemical characterization, and subcellular localization of allantoate amidohydrolases from Arabidopsis and soybean.* Plant Physiol, 2008. **146**(2): p. 418-30.
5. Agarwal, R., S.K. Burley, and S. Swaminathan, *Structural analysis of a ternary complex of allantoate amidohydrolase from Escherichia coli reveals its mechanics.* J Mol Biol, 2007. **368**(2): p. 450-63.
6. van der Drift, C., F.E. de Windt, and G.D. Vogels, *Allantoate hydrolysis by allantoate amidohydrolase.* Arch Biochem Biophys, 1970. **136**(1): p. 273-9.
7. Xu, Z., F.E. de Windt, and C. van der Drift, *Purification and characterization of allantoate amidohydrolase from Bacillus fastidiosus.* Arch Biochem Biophys, 1995. **324**(1): p. 99-104.
8. Wu, C.H., E.J. Eisenbraun, and E.T. Gaudy, *Enzymatic degradation of ureidoglycine by Pseudomonas acidovorans.* Biochem Biophys Res Commun, 1970. **39**(5): p. 976-82.
9. Muratsubaki, H., K. Satake, and K. Enomoto, *Enzymatic assay of allantoin in serum using allantoinase and allantoate amidohydrolase.* Anal Biochem, 2006. **359**(2): p. 161-6.
10. Gravenmade, E.J., G.D. Vogels, and C. Van der Drift, *Hydrolysis, racemization and absolute configuration of ureidoglycolate, a substrate of allantoicase.* Biochim Biophys Acta, 1970. **198**(3): p. 569-82.
11. Serventi, F., et al., *Chemical basis of nitrogen recovery through the ureide pathway: formation and hydrolysis of S-ureidoglycine in plants and bacteria.* ACS Chem Biol. 2010 Jan 15. [Epub ahead of print]
12. Rudd, K.E., *Linkage map of Escherichia coli K-12, edition 10: the physical map.* Microbiol Mol Biol Rev, 1998. **62**(3): p. 985-1019.
13. Gouet, P., et al., *ESPript: analysis of multiple sequence alignments in PostScript.* Bioinformatics, 1999. **15**(4): p. 305-8.
14. Dunwell, J.M., et al., *Evolution of functional diversity in the cupin superfamily.* Trends Biochem Sci, 2001. **26**(12): p. 740-6.
15. Agarwal, G., et al., *Structure-based phylogeny as a diagnostic for functional characterization of proteins with a cupin fold.* PLoS One, 2009. **4**(5): p. e5736.
16. Raymond, S., et al., *Crystal structure of ureidoglycolate hydrolase (AllA) from Escherichia coli O157:H7.* Proteins, 2005. **61**(2): p. 454-9.
17. Lewis, M.J. and H.R. Pelham, *SNARE-mediated retrograde traffic from the Golgi complex to the endoplasmic reticulum.* Cell, 1996. **85**(2): p. 205-15.
18. Kitagawa, M., et al., *Complete set of ORF clones of Escherichia coli ASKA library (a complete set of E. coli K-12 ORF archive): unique resources for biological research.* DNA Res, 2005. **12**(5): p. 291-9.
19. Bolchi, A., S. Ottonello, and S. Petrucco, *A general one-step method for the cloning of PCR products.* Biotechnol Appl Biochem, 2005. **42**(Pt 3): p. 205-9.
20. Abel, S. and A. Theologis, *Transient transformation of Arabidopsis leaf protoplasts: a versatile experimental system to study gene expression.* Plant J, 1994. **5**(3): p. 421-7.

Chapter 4

S-UREIDOGLYCOLATE HYDROLASE

S-Ureidoglycolate hydrolase

ABSTRACT

Ureidoglycine hydrolysis produces ureidoglycolate, which can be metabolized to glyoxylate by the enzymes ureidoglycolate urea-lyase (EC 4.3.2.3) or ureidoglycolate amidohydrolase (EC 3.5.3.19). Both a ureidoglycolate amidohydrolase (EC 3.5.3.19) and a ureidoglycolate urea-lyase (EC 4.3.2.3) have been purified from French bean and other leguminous species. Up till now is not known the gene encoding for the ureidoglicolate hydrolase in *A.thaliana*. Here are shown the isolation and purification of the *E. coli* ureidoglycolate hydrolase (AllA) homolog gene of Arabidopsis. This protein was tested for the ability to hydrolyze S-ureidoglycolate. The enzyme, however, is not able to produce neither urea not ammonia from ureidoglycolate.

INTRODUCTION

Ureidoglycolate can be metabolized to glyoxylate by either ureidoglycolate urea-lyase (EC 4.3.2.3) or ureidoglycolate aminohydrolase (EC 3.5.3.19). These activities differ in the nature of the nitrogen compound produced: ureidoglycolate aminohydrolases yield ammonium, whereas ureidoglycolate urea-lyase release urea. [1] (Figure 4.1). Both ureidoglycolate aminohydrolase and ureidoglycolate urea-lyase have been purified from plant leguminous species [2] [3] and green algae [4].

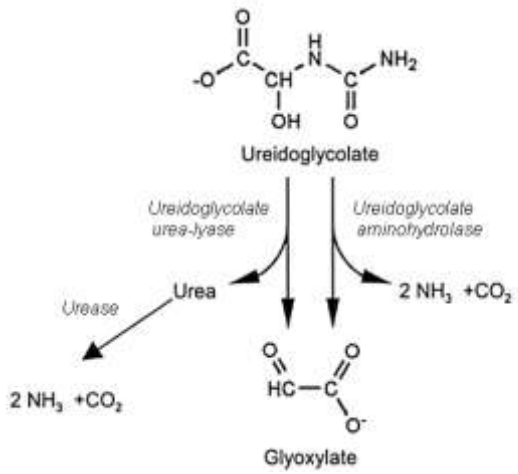

Figure 4.1 Degration of ureidoglycolate to gliyoxylate. Ureidoglycolate can be hydrolyzed by two different enzymes: ureidolycolate urea-lyase and ureidoglycolate aminohydrolase (Adapted from Todd and Polacco, 2004).

RESULTS AND DISCUSSION

Identification of the putative *Arabidopsis* ureidoglycolate hydrolase

Using as a query the *E. coli* ureidoglycolate hydrolase (AllA; YP_002401636.1) and running a BLAST on the *Arabidopsis* proteome it was found a putative *Arabidopsis* ureidoglycolate hydrolase (UGH) with a marginally significant e value. This protein share 21% of identity with the *E. coli* ureidoglycolate hydrolase. Pfam indicates that this protein belongs to the ureidoglycolete hydrolase family, even if with a marginally significant e value too (figure 4.2).

Family	Description	Entry type	Clan	Envelope		Alignment		HMM		Bit score	E-value	Predicted active sites
				Start	End	Start	End	From	To			
Ureidogly_hydro	Ureidoglycolate hydrolase	Family	n/a	80	193	131	174	111	153	15.6	0.0057	n/a

Figure 4.2 Pfam output. UGH belongs to the ureidoglycolate hydrolase family.

In *Arabidopsis* are present three paralog proteins of the putative ureidoglycolate hydrolase produced from genes that lie on chromosome two in a row (loci At2g35810, At2g35820, At2g35830).
All these proteins have unknown function and the second and the third genes share the same regulative elements (Figure 4.3).

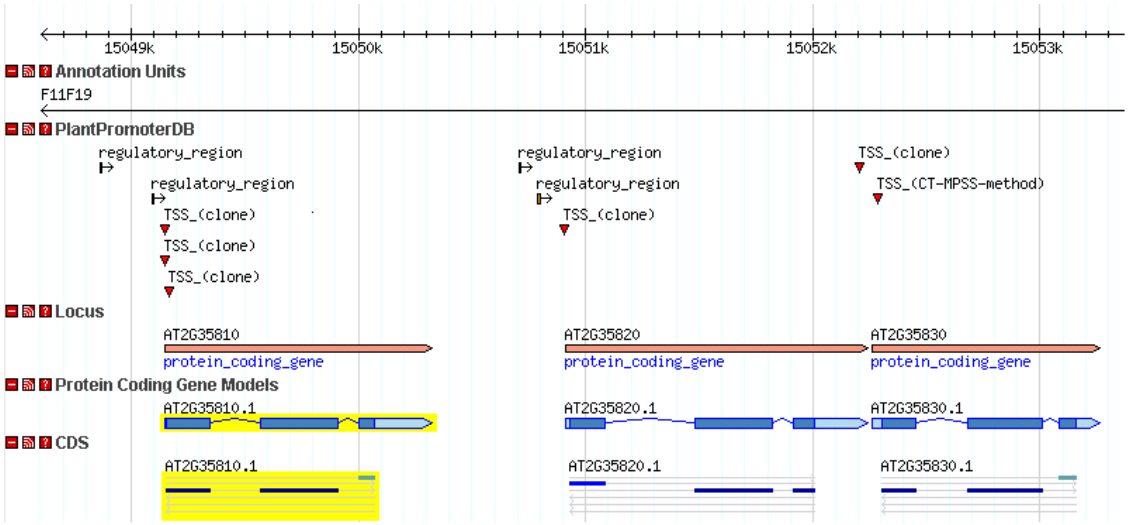

Figure 4.3 Gene position of *A.thaliana* ureidoglycolate hydrolase homologs on chromosome two.

The proteins coded by the genes located at At2g35820 and At2g35830 have respectively 75% and 91% of identity with the protein coded by the gene in the locus At2g35810. (figure 4.2).

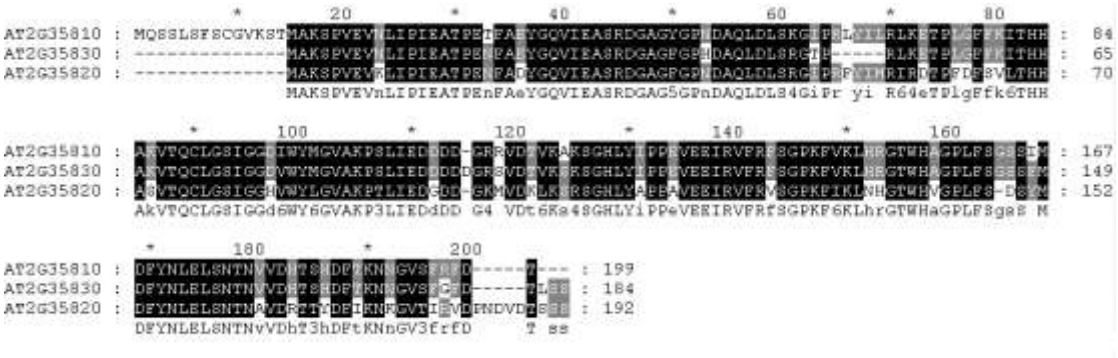

Figure 4.2 Alignment of three paralog proteins of *A. thaliana* with putative ureidoglycolate hydrolase function.

Expression profile of the putative ureidoglycolate hydrolase

The expression profile of At2g35810 obtained using the *Arabidopsis* eFP Browser shows that RNAs produced from this gene are present in leaves (overall cauline leaves), senescent cotiledons and in seeds during germination but not in dry seeds (figure 4.3) consistent with the expression of the ureide pathway proteins.

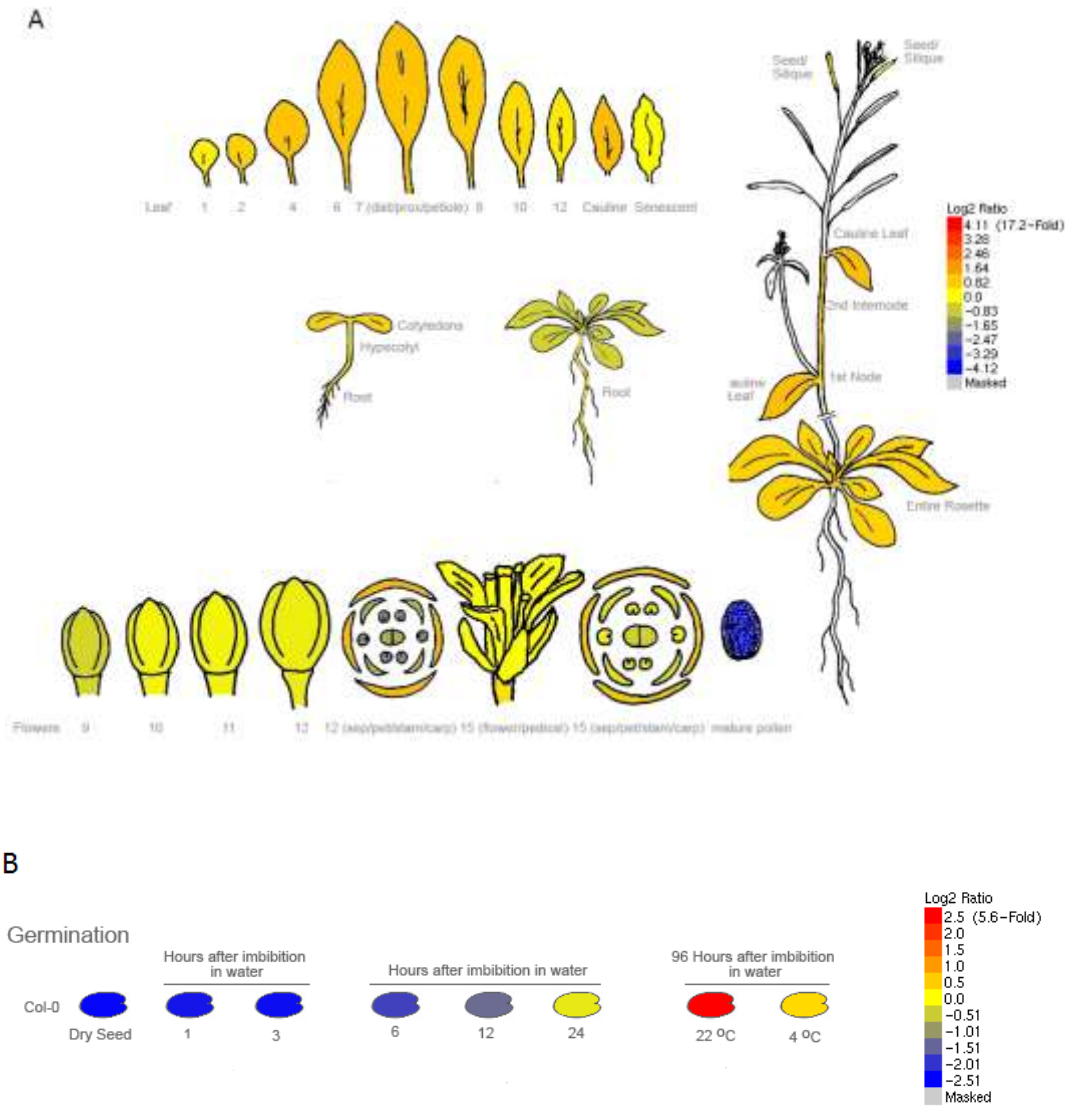

Figure 4.3 Expression pattern of At2g35810 A) developmental map B) seed germination.

Cloning and expression of the putative ureidoglycolate hydrolase

The protein coded by the gene present in the locus At2g35810 was amplified and cloned since it has an higher number of ESTs associated than the other proteins.
From the alignment analysis of the three homolog proteins of *Arabidopsis thaliana* (figure 4.2) it was decided to delete the 5' portion of the coding sequence because it hasn't no correspondence with the other two proteins and the presence of this N-terminal portion can be due to an incorrect prediction of the initial metionine. UGH was amplified from cDNA and amplicons were cloned in pET28 for the expression of the recombinant protein in *E. coli*.
UGH was purified using an affinity metal chromatography and tested for the ability to produce ammonia or urea and glyoxylate from S-ureidoglycine (figure 4.4). The assay used is the same as that used for S-ureidoglycine hydrolase. It consists of a coupled assay in which the ammonia produced from the hydrolysis of ureidoglycine is used by glutamate dehydrogenase to convert α-ketoglutarate in glutamate in a NADPH-dependent manner. The difference in assorbance due to the oxidation of NADPH to $NADP^+$ is monitored at 340 nm with a spectrophotometer.

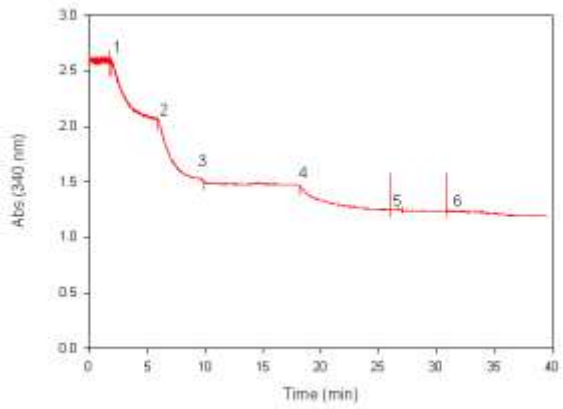

Figure 4.4 Time courses of ammonia release using a coupled assay with glutamate dehydrogenase.
Time course of ammonia release from allantoate (0.5mM) monitored spectrophotometrically using a coupled assay with glutamate dehydrogenase. The reaction was initiate by the addition of 0.075 mM allantoate (1) to a solution containing 0.13 µM AllC and 0.1 mM $MnCl_2$. Successive addition of AtYlbA (2), UGH (3) and urease (4). The addiction of Mg, Zn, Cu, Ni, Co (5 and 6) did not activate the enzyme.

UGH is not able to catalyze the conversion of S-ureidoglycolate to glyoxylate neither producing ammonia nor urea.
Munoz and co-workers indicate that the activity of the purified ureidoglycolate urea-lyase from French bean (*Phaseolus vulgaris* L.) is completely dependent on manganese and asparagine [3] and that optimum pH for the ureidoglycolate urea-lyase activity from chickpea (*Cicer arietinum*) is

between 7 and 8 [1]. The UGH enzyme from *A. thaliana* is inactive when tested either in presence of asparagine or at different pH.

In November 2009 Werner et al indentified in another protein from *A.thaliana* the enzyme ureidoglycolate amidohydrolase [5]. Differing from other plants like French bean and chickpea, the *Arabidopsis* enzyme release ammonia and not urea.

METHODS

Cloning and production of recombinant UGH

UGH was amplified from cDNA derived from total *Arabidopsis* RNA with the following primer forward 5' – ATCGGTCCGGGTGTCAAGTCAACGATGGCG-3' and reverse 5'-TACGGACCGTCCATTATTCTTCTTAGGTGTC-3'. All the primers bore 5'-tails such that the amplification products contained CpoI target sequences near to both ends, necessary for the subcloning in the expression vector pET28-CpoI.

Amplicons were cloned into pBluescript KS, plasmids were then inserted into XL1B E. coli cells (Stratagene) and the inserts were sequence-verified. PBluescript KS-UGH was subsequently treated with CpoI to extract the fragments corresponding to the amplified CDS, ready for subcloning into the expression vector pET28- CpoI. This plasmid is a derivative of pET28 (Novagen) modified to present a single CpoI restriction site in the cloning region, downstream to a sequence encoding a hexa-histidine tag (Angelo Bolchi, unpublished). *E. coli* BL21 (DE3) condon plus cells (Stratagene) transformed with UGH-pET28-CpoI were incubated at 37°C in a LB minimal medium until they reached the optical density of 0.6 at 600 nm. Expression was induced by adding 1mM IPTG and transferring the culture at 30°C for 3 hours.

Cells from 10 ml of culture were lysed by sixty 30'' bursts of sonication in 1 ml of 50 mM sodium phosphate, 300 mM NaCl, 10% glycerol, 0.005% Tween 20, pH 7.5. Proteins were purified by TALON Metal Affinity Resin (Clontech) and eluted by adding 100 mM imidazole.

Biochemical assays

Ammonia release by the AllC reaction was determined spectrophotometrically using a coupled assay with glutamate dehydrogenase (GDH) [6, 7]. The typical incubation mixture consisted of 1 ml of 0.2 M Tris-HCl buffer, pH 8.5, with 0.3 mM NADPH, 2.5 mM α-ketoglutarate, 4.12 units of GDH from *Proteus sp* (Sigma), 100 µM MnCl2, and 6 µg AllC. The reaction was initiated by the addition of allantoic acid (0.15 mM) and the decrease in absorbance at 340 nm due to the oxidation of NADPH was recorded. Recombinant AtYlbA (6 µg) was added after the fast phase of the AllC reaction. UGH (6 µg) was added (pre-incubate or not with 10 mM Asn) after the fast phase of AtYlbA reaction.

Different reaction pH was tested using as a buffer: potassium phosphate pH 7, 7.6 or Tris pH8 or 8.5. The production of urea was excluded introducing urease at the end of UGH reaction.

REFERENCES

1. Munoz, A., et al., *Urea is a product of ureidoglycolate degradation in chickpea. Purification and characterization of the ureidoglycolate urea-lyase.* Plant Physiol, 2001. **125**(2): p. 828-34.
2. Wells, X.E. and E.M. Lees, *Ureidoglycolate amidohydrolase from developing French bean fruits (Phaseolus vulgaris [L.].).* Arch Biochem Biophys, 1991. **287**(1): p. 151-9.
3. Munoz, A., et al., *Degradation of ureidoglycolate in French bean (Phaseolus vulgaris) is catalysed by a ubiquitous ureidoglycolate urea-lyase.* Planta, 2006. **224**(1): p. 175-84.
4. Piedras, P., M. Aguilar, and M. Pineda, *Uptake and metabolism of allantoin and allantoate by cells of Chlamydomonas reinhardtii (Chlorophyceae)*. 1998, Taylor & Francis. p. 57 - 64.
5. Werner, A.,K., Romeis, T.,and Witte C., P. *Ureide catabolism in Arabidopsis thaliana and Escherichia coli Nature Chemical Biology* **6**, 19 - 21 (2010)
6. van der Drift, C., F.E. de Windt, and G.D. Vogels, *Allantoate hydrolysis by allantoate amidohydrolase.* Arch Biochem Biophys, 1970. **136**(1): p. 273-9.
7. Muratsubaki, H., K. Satake, and K. Enomoto, *Enzymatic assay of allantoin in serum using allantoinase and allantoate amidohydrolase.* Anal Biochem, 2006. **359**(2): p. 161-6.

Appendices

SUMMARY

Ureide, allantoin and allantoate, are nitrogen-rich compounds derived from purine catabolism. While birds, insects and most primates including humans, eliminate uric acid to get rid of excess nitrogen, for many others organisms the recovery of the purine ring nitrogen is vital. In this organisms uric acid is converted into ammonia and glyoxylate via allantoin and allantoate allowing the rescue of nitrogen atoms. The aim of this study was to investigate on chemical basis of nitrogen recovery through the ureide pathway in *A. thaliana.* The state of the art in the ureide metabolism is described in chapter one. In chapter two is described the gene involved in S-allantoin biosynthesis. This gene (TTL) catalyzes two enzymatic reaction leading to the steroselective formation of S-allantoin: hydrolysis of hydroxyisourate (HIU) through a C-terminal Urah domain and decarboxylation of OHCU through a N-terminal Urad domain. In other organisms but plants and few some organisms these domains are present in two different gene units. Besides this peculiarity this gene produce two isoforms of mRNA by differential splicing. The two proteins generated have similar catalytic activity *in vitro* but different *in vivo* localisation: TTL^{1-} localizes in peroxisomes whereas TTL^{2-} localizes in the cytosol. Transcripts deriving from the two splice variants are present in a similar proportion in various *Arabidopsis* tissues but in floral buds, where TTL^{2-} is prevalent. Analysis of TTL transcripts in various plants indicate that similar splice variants are present in monocots and dicots. The peroxisomal enzyme must be the S-allantoin synthase because HIU is an unstable substrate that should be only produced in these organelles trough the oxidation of urate by urate oxidase. The cytoplasmic enzyme could be the one that interact with the kinasic domain of brassinosteroid receptor as reported in another study.

In chapter three is reported the identification and the characterization of a gene of unknown function to be a S-ureidoglycine hydrolase. Ureidoglycine is produced by allantoate amidohydrolase, a manganese-dependent enzyme found in plants and bacteria. Ureidoglycine spontaneously decays into urea and glyoxylate *in vitro*, while living cells produce S-ureidoglycolate. S-ureidoglycine amidohydrolase catalyze the Mn-dependent release of ammonia through hydrolysis of S-ureidoglycine yields S-ureidoglycolate. This enzyme in plants is localized, like allantoate amidohydrolase, in the endoplasmic reticulum.

In chapter four, is described the cloning, over-expression and purification of the *Arabidopsis* homologous of *E. coli ureidoglycolate hydrolase gene.* Activity assay on this protein demonstrated that even if the protein are homologues the putative *Arabidopsis* ureidoglycolate hydrolase has not that function. In a recent publication (Werner et al, November 2009) the ureidoglycolate hydrolase function was associated with another *Arabidopsis* protein.

RIASSUNTO

Le ureidi, allantoina e allantoato, sono delle molecole ricche di azoto che derivano dal catabolismo delle purine. Alcuni organismi come uccelli, insetti e molti primati tra cui l'uomo eliminano l'eccesso di azoto sotto forma di acido urico, mentre per altri organismi il recupero degli atomi di azoto contenuti nelle purine può essere di vitale importanza. In questi organismi l'acido urico è convertito in ammonio e gliossilato passando attraverso gli intermedi allantoina e allantoato, permettendo il completo recupero dei quattro atomi di azoto contenuti nelle basi puriniche.

Questo lavoro ha avuto lo scopo di studiare le basi molecolari del recupero dell'azoto lungo la via metabolica delle ureidi in *A.thaliana*. Lo stato dell'arte riguardo a questo argomento è descritto nel capitolo uno. Nel capitolo due è riportato lo studio che riguarda il gene coinvolto nella biosintesi della S-allantoina. Questo gene (TTL) catalizza i due passaggi enzimatici che portano alla formazione di allantoina stereoselettiva a partire da idrossiisourato(HIU): idrolisi dell'HIU, attraverso un dominio C-terminale (Urah), e decabossilazione del prodotto, 2-osso-4-hydrossi-4-carbossi-5-ureidoimidazolina (OHCU), attraverso un dominio N-terminale (Urad). In altri organismi diversi dalle piante, questi domini sono presenti come singoli polipeptidi codificati da geni diversi. Oltre alla peculiarità di essere un gene con un prodotto bifunzionale, quello di *Arabidopsis* produce un trascritto che va incontro a splicing alternativo che dà origine due isoforme di RNA. Le proteine generate dalla traduzione di queste isoforme hanno attività simile *in vitro*, ma si localizzano in compartimenti cellulari diversi *in vivo*. TTL^{1-} viene importata nel perossisoma, mentre TTL^{2-} resta nel citosol. I trascritti che derivano dallo splicing alternativo sono presenti in quantità simili nei vari tessuti di *Arabidopsis*, con l'eccezione dei boccioli dove l'isoforma più corta è circa cinque volte maggiore rispetto a quella più lunga. L'analisi delle EST di diverse piante indica che lo splicing alternativo, sebbene non presente in tutte le piante, è conservato nelle monocotiledoni e dicotiledoni.

L'enzima perossisomiale deve essere quello adibito alla conversione di HIU in allantoina ed è stato ribattezzato S- allantoina sintasi, poiché l'HIU è un substrato instabile prodotto dall'urato ossidasi nel perossisoma. La proteina citoplasmatica, sebbene sia in grado di formare allantoina, potrebbe essere implicata nella regolazione della crescita della pianta come interattore della porzione chinasica del recettore di membrana dei brassinosteroidi come riportato in studi precedenti (Nam et Lee, 2004).

Nel capitolo tre è riportata la caratterizzazione di un gene a funzione ignota, identificato come S-ureidoglicina idrolasi.l'ureidoglicina viene prodotta lungo il pathway delle ureidi dall'enzima Mn-dipendente allantoato amido idrolasi. Questa molecola subisce degradazione spontanea ad urea e gliossilato *in vitro*, ma viene trasformata in S-ureidoglicolato *in vivo*. L'enzima S-ureidoglicina amidoidrolasi catalizza l'idrolisi manganese-dipendente dell'ureidoglicina formando ureidoglicolato e ammonio. In *Arabidopsis* questo enzima si trova, così come l'allantoato amido idrolasi nel reticolo endoplasmatico.

Nel capitolo quattro sono descritti il clonaggio, la sovra-espressione e la purificazione del gene di *Arabidopsis* omologo all'ureidoglicolato idrolasi di *E. coli*. I saggi di attività su questa putativa

ureidoglicolato idrolasi hanno dimostrato che questa proteina sebbene omologa a quella a funzione nota di batterio, non è capace di idrolizzare l'ureidoglicolato. In una recente pubblicazione (Werner et al., novembre 2009) è stata identificata l'ureidoglicolato idrolasi di *Arabidopsis*, in una proteina omologa all'allantoato amido idrolasi di pianta piuttosto che all'ureidoglicolato idrolasi batterica.

CURRICULUM VITAE

I was born on October 9th , 1981 in Locri (RC), Italy. I went to high school in Locri (Liceo Scientifico Zaleuco) from 1995 to 2000. At the University of Parma I studied first Biotechnology (Bachelor Degree) with a final mark of 108/110, then Molecular Biology (Master Degree) and in September 2006 I graduated *cum laude*. From January 2007 to December 2009 I specialized in Biochemistry and Molecular Biology, as PhD student, in the laboratory of Professor Riccardo Percudani at the Department of Biochemistry and Molecular Biology. The aim of the work was to investigate on chemical basis of nitrogen utilization through the ureide pathway in *A.thaliana*.The work resulted in this thesis and two manuscripts submitted two international scientific journals. During this three years I also contributed to the work of Professor Alessio Peracchi that led to the publication of the article *Recombinant production of eight human cytosolic aminotransferases and assessment of their potential involvement in glyoxylate metabolism.*

LIST OF PUBBLICATION

1. Donini, S., Ferrari, M., Fedeli, C., Faini, M., **Lamberto, I.,** Marletta, A.S., Mellini, L., Panini, M., Percudani, R., Polleggioni, L., Caldinelli, L., Petrucco, S., Peracchi, A., *Recombinant production of eight human cytosolic aminotransferases and assessment of their potential involvement in glyoxylate metabolism.* Biochem J, 2009. 422(2): p. 265-72.

2. Serventi, F., Ramazzina, I., **Lamberto, I.,** Puggioni, V., Gatti, R., Percudani, R., *Chemical basis of nitrogen recovery through the ureide pathway: formation and hydrolysis of S-ureidoglycine in plants and bacteria. ACS Chem Biol. 2010 Jan 15. [Epub ahead of print]*

3. **Lamberto, I.,** Percudani, R., Gatti, R., Folli, C., Petrucco, S., *Alternative splicing of TTL (S-allantoin synthase) regulates stereoselective ureide synthesis in plant peroxisomes.* Submitted to Plant Cell